



DESIGN AND ANALYSIS OF A COMPRESSED AIR VEHICLE

A thesis submitted to the department of Mechanical and Production Engineering (MPE), Islamic University of Technology (IUT), in the partial fulfillment of the requirement for degree of Bachelors of Science in Mechanical Engineering.

Supervised By

Prof. Dr. Md. Nurul Absar Chowdhury

Prepared By

Khalil I A Shatat (151458)

Hassn A. H. Haniyeh (151456)

Amro A A Alawawda (160011087)

Abdallah N M Abukashef (160011091)

Sohaib O A Alqedra (151462)

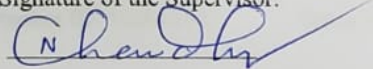
Said A B Alfarra (151463)

March-2021

CERTIFICATE OF RESEARCH:

The thesis title "**Design and Analysis of a Compressed Air Vehicle**" submitted by Khalil I A Shatat (151458), Hassn A. H. Haniyeh (151456), Sohaib O A Alqedra (151462), Said A B Alfarra (151463), Abdallah N M Abukashef (160011091) and Amro A A Alawawda (160011087) has been accepted as satisfactory in partial fulfillment of the requirement for the Degree of Bachelor of science in Mechanical and Production Engineering on March, 2021.

Signature of the Supervisor:



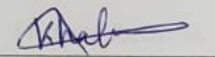
Prof. Dr. Md. Nurul Absar Chowdhury

Department of Mechanical and Production Engineering.

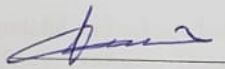
CANDIDATE'S DECLARATION:

It is hereby declared that this thesis or any part of it has not been submitted elsewhere for the award of any degree or diploma.

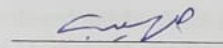
Signatures of the Candidates.



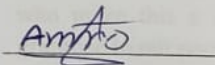
Khalil I A Shatat
Student ID:151458



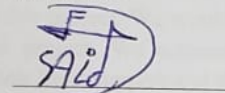
Hassn A. H. Haniyeh Student
ID:151456



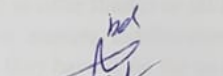
Sohaib O A Alqedra
Student ID: 151462



Amro A A Alawawda
Student ID: 160011087

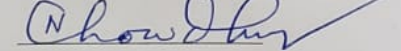


Said A B Alfarra
Student ID:151463



Abdallah N M Abukashef
Student ID:160011091

Signature of the Supervisor:



Prof. Dr. Md. Nurul Absar Chowdhury

Department of Mechanical and Production Engineering.

Department of Mechanical & Production Engineering (MPE) Islamic University of
Technology (IUT), OIC Board Bazar, Gazipur Bangladesh.

ACKNOWLEDGEMENT:

First and foremost, we feel grateful and acknowledge our profound indebtedness to Prof. Dr. Md. Nurul Absar Chowdhury, Professor, Department of Mechanical and Production Engineering, IUT. His endless patience, scholarly guidance, continual encouragement, constant and energetic supervision, constructive criticism, valuable advice at all stage has made it possible to complete this project. We would also like to offer thanks to all friends who make this a successful project. We acknowledge our sincere indebtedness and gratitude to our parents for their love, support and the efforts they have done for us so far.

We seek excuse for any errors that might be in this report despite of our best efforts.

Table of Contents

INTRODUCTION	7
1.1 Problem statement	7
1.1.1 Vehicle emissions and their impact on human health	8
1.1.2 Vehicle emissions and their impact on environment	10
1.2 Emissions control in engines	10
1.2.1 Catalytic convertor	10
1.2.2 Exhaust gas recirculation (EGR) valve	11
1.2.3 Evaporative control system	11
1.2.4 Air injection.....	11
1.2.5 Engine modifications.....	11
1.3 Purpose and Significance of the thesis	12
LITRATURE REVIEW	13
2.1 The Technology of Compressed Air Engine.....	13
2.2 Development of Compressed Air Engine.....	14
2.3 Advantages of Compressed Air vehicles.....	15
2.4 Drawback of compressed Air Engines	16
METHODOLOGY, CALCULATIONS AND SIMULATION	17
3.1 The Pneumatic Setup.....	17
3.2 The control unit	18
3.2.1 Controlling the 4 ways 5 ports solenoid valve	18
3.2.2 The steering system control.....	24
3.3 The crankshaft design.....	30
3.3.1 Crank shaft material	31
3.3.2 Crank shaft analysis and assumptions	31
3.3.3 Analyzing the crank shaft at top dead center position.....	31
3.3.4 Analyzing the crank shaft when it is subjected to maximum torsional moment ...	34
3.3.5 Testing the crank shaft design using finite element method.....	38
3.4 Connecting rod design.....	41
3.4.1 Connecting rod material	42
3.4.2 Connecting rod dimensions	42
3.4.3 The ends of the connecting rod.....	44
3.4.4 Testing the crank shaft design using finite element method.....	47

3.5	Chassis design	52
3.6	Differentials.....	57
3.7	bearings design	61
CONCLUSION		63
References		64

CHAPTER ONE

INTRODUCTION

1.1 Problem statement

The exhausted gas from the vehicle contains a lot of harmful chemical compounds. The presence of these contaminants have a deleterious impact on human health, welfare and the environment. These pollutant substances are considered to be responsible for the photochemical smog, acid rain, a reduced atmospheric visibility and the global warming. Air pollution has been recognized as a very complex societal problem where its cause and effect relationships have been reasonably deductive.

The major cause of the air pollution is combustion. When it occurs, the hydrogen and carbon from the fuel reacts with the oxygen in the air producing heat, light, carbon dioxide and water vapor. Some side products of this reaction such as nitrogen oxides, carbon monoxide, sulfur oxides, fly ash and hydrocarbons are formed due to impurities in the fuel, poor fuel-to-air ratio, too high or too low combustion temperature. These chemical compounds are air pollutants.

The industrial revolution had the abundant share of polluting the air. Burning the coal for the factories and power generation was a major source of the chemical pollutant of the atmosphere. Which appears as smog (smoke and fog) in the air.

A similar air condition was reported in 1995 in the United States. The national air quality standards for specific air pollutants were violated in several regions and areas. These locations included 77 areas for ozone, 36 for carbon monoxide, 82 for particulate matter, 43 for sulfur dioxide, 11 for lead and one for nitrogen dioxide.

The air pollution used to be an intractable issue for most of the world before the 20th century. In 1200s, King Edward I of England tried to find a solution for the polluted atmosphere of London by banning the use of sea coal. King Edward II ordered the execution of anyone found burning coal while the British Parliament was meeting. Starting from the authority of Richard II (1377 -1399) and later under Henry V (1413-1422), England began to issue policies to regulate the use of coal in order to reduce the emissions affecting the air quality.

With each passing decade, the information on air quality allows for continuously improving decisions that have led to a much cleaner atmosphere by making pollution sources of earlier decades become obsolete and are replaced by processes and equipment that produce less pollution. The improvement has been remarkable, mainly in the health-related criteria air pollution.

Since 90% of the emissions are gases, the suitable solution seems to reduce the amount of the harmful gaseous particles from the effluent gas. Several ways have been developed and

improved to treat the exhausted gases after the combustion. One of them is to adsorb the pollutant species on the surface of a solid adsorbent based on the ability of some solids to remove components from a flow stream using Van Der Waals force of attraction. Another method to reduce the impurities in the air flow is absorption of the species in a liquid solvent where the dirty effluent gas is brought in contact with a scrubbing liquid. The contaminated gas is absorbed in the liquid then the contaminated liquid is changed. The pollutant might also be oxidized by combusting the flue gas by means of direct flame or catalytic incineration to alter the reaction products to another form which is not a pollutant. The last approach to control the contaminated exhaust gas is to reduce the concentration of the diluents from the fuel or the oxidant using filters.

The first effort at controlling pollution from automobiles was the positive crankcase ventilation (PCV) system. This draws crankcase fumes heavy in unburned hydrocarbons a precursor to photochemical smog into the engine's intake tract so they are burned rather than released them to the atmosphere. Positive crankcase ventilation was first installed on a widespread basis by law on all new 1961-model cars first sold in California, USA. The following year, New York required it. By 1964, most new cars sold in the U.S. were so equipped, and PCV quickly became standard equipment on all vehicles worldwide.

1.1.1 Vehicle emissions and their impact on human health

The composition of the exhaust emissions varies depending on air-to-fuel ratio, speed, combustion efficiency, and the fuel purity. However, there are some contaminants usually present in the flue gas; such as hydrocarbons, nitrogen oxides, carbon monoxide, carbon dioxide, photochemical oxidants, particulate matter, and sulfur oxide. These pollutants affect negatively the human health and the environment.

Effect of hydrocarbons, nitrogen oxides and photochemical oxidants on human health

The emission of hydrocarbons is related to the combustion efficiency. That occurs when unburned fuel vaporizes and leaves the combustion chamber with the exhaust gas. Though the hydrocarbons are not considered as pollutants as a general list, a huge number of specific hydrocarbons are identified as hazardous pollutants and studies of certain hydrocarbon classes found them responsible for some types of cancer.

The atmospheric air contains nitrogen oxides in different forms. These include nitric oxide (NO), nitrogen dioxide (NO₂), nitrous oxide (N₂O), nitrate ion (NO₃), dinitrogen trioxide (N₂O₃), dinitrogen tetroxide (N₂O₄) and dinitrogen pentoxide (N₂O₅). The Nitric Oxide (NO) and Nitrogen dioxide (NO₂) are usually referred by the term nitrogen oxides (NO_x). The exposure to NO₂ was found to be a reason to chronic obstructive pulmonary disease (COPD).

The combination of hydrocarbons and nitrogen oxides in presence of the sunlight form photochemical oxidants including ozone (O₃) which affects the human health. The photochemical oxidants refer to the oxidizing agents that can oxidize the potassium

iodide, peroxyacetyl nitrate, Formic acid, hydrogen peroxide. These oxidants affect the well-being of human by causing severe eye, nose and throat irritation, chest constriction and severe coughing and inability to concentrate at high concentrations.

Effect of carbon monoxide on human health

As a source of the hydrocarbons, the exhausted unburned fuel also contains carbon monoxide (CO) which can stay in the atmosphere up to 4 months. During the period of 1970 to 1980 in the U.S., about 70% of the carbon monoxide emissions were from the highway vehicles. Although a small amount of carbon monoxide is discharged from a vehicle due to the emission control systems, the danger presents from the number of vehicles available on the road and the distance the travel.

Besides participating in the photochemical reactions, the carbon monoxide causes physiological and pathological changes and toxic inhalant that prevent the body tissues from necessary oxygen.

The carbon monoxide is a direct motive of the carboxyhemoglobin (COHB) when it combines with the hemoglobin which leads to oxygen deficiency in the body.

Effect of particulate matter on human health

The term particulate matter refers to the solid or liquid particles larger than $0.0002\ \mu\text{m}$ but less than $500\ \mu\text{m}$ in diameter. 20 to 60% of the emitted particles are between 0.01 and $2.5\ \mu\text{m}$. Inhaling these particulate matters alone or combined with another pollutants can severely damage the respiratory organs after they are deposited in the lungs. The danger of the particulate matters is subjected to their inherent chemical or physical characteristics and it might as well obstruct one or more mechanisms which normally clears the respiratory tract in addition to ability of the liquid particulates to absorb toxic matters or adsorb them in case of solid particles.

Effect of sulfur oxides on human health

The sulfur dioxide and trioxide have the highest concentrations in the atmosphere among all sulfur oxides. The combination of sulfur oxides with particulate matters and moisture form a serious health hazard.

Bronchoconstriction is a result from the exposure to sulfur dioxide which is a condition when the smooth muscles of the bronchus contracts. This muscle contraction causes the bronchus to narrow and restrict the amount of air passing into and out of the lungs.

1.1.2 Vehicle emissions and their impact on environment

Along with harming human health, air pollution can cause a variety of environmental effects:

Acid rain

Acid rain is defined as the wet and dry deposition of acidic substances from the atmosphere. These acids fall to earth in form of rain, snow, cloud water droplets, or solid particles. These acids are formed from nitrogen oxides and sulfur oxides exhausted to the atmosphere after the combustion of fuel. The danger of acid rain is it damages trees and causes soils and water bodies to acidify, making the water unsuitable for some fish and other wildlife.

Ozone depletion

Ozone (O₃) is normally present at the stratosphere (Earth's upper atmosphere). It forms a layer that protects life on earth from the sun's harmful ultraviolet (UV) rays. However, its presence at ground level is considered harmful. Thinning of the protective ozone layer increases the amounts of UV radiation that reaches the Earth. UV can also damage sensitive crops, such as soybeans, and reduce crop yields. The ozone depletion is caused by the nitric oxide (NO).

Global warming and climate change

The Earth's atmosphere temperature is balanced naturally by receiving heat from sun and releasing infrared radiation that sends heat back into space. This "greenhouse effect" keeps the Earth's temperature stable. The increasing concentration of carbon dioxide CO₂ limits the travel of the infrared radiation as CO₂ absorbs infrared. As a result, the temperature of the Earth is increasing, resulting in the melting of ice, icebergs, and glacier. Many scientists believe that global warming could have significant impacts on human health, agriculture, water resources, forests, wildlife, and coastal areas.

1.2 Emissions control in engines

Since recognizing the major effects of car emissions on the air pollution, a lot of method, techniques and engine modifications have been developed to reduce the amount of pollutants that vehicles engine produce.

1.2.1 Catalytic convertor

One way to control the engine emissions is to provide more air from the combustion to occur. The additional space is called catalytic convertor. This convertor is placed in the exhaust system and platinum or palladium shaped like honeycomb is used as catalysts to speed up the reactions. When carbon monoxide or hydrocarbons passes over the catalyst, they are oxidized to carbon dioxide and water vapor.

This process generates heat proportionally related to the dirtiness of the exhaust gas. So in extreme conditions, the heat generated might destroy the catalytic converter.

1.2.2 Exhaust gas recirculation (EGR) valve

The nitrogen oxides are produced when the temperature in the combustion chamber is excessively high. The EGR valve is used to redirect a limited amount of the exhaust gas back to the intake system to dilute the air-fuel mixture. This process has an adverse impact on the efficiency of the engine. EGR valve does not take any action when the engine starts and when full engine power is needed.

1.2.3 Evaporative control system

The evaporative control system is used to trap the fuel vapor from the fuel tank and the carburetor due to the nature of fuel. The fuel vapor is collected in charcoal canister then drawn to the engine when it starts to be burned with the fuel-air mixture.

The fuel vapor is sent to the intake system with the help of the engine vacuum. A purge valve is used to regulate the vapor flow into the engine.

The drawback of this system is that the purge valve fails and the vapors will go directly to the intake system unregulated.

1.2.4 Air injection

The air injection system was developed to completely burn the unburned fuel particles in the exhaust flow which is a primary source of the hydrocarbons. Introducing oxygen to the heat and unburned fuel in the exhaust manifold ignites these fuel particles.

1.2.5 Engine modifications

In addition to the separated emission control systems, some improvements can be implemented to the engine to reduce the amount of produced pollutants. However, these modifications depend on the engine type.

For SI engines, the carburetor can be completely replaced by multi-port fuel injection system. The fuel supply to the cylinder can be accurately regulated using electronic engine management by sensing different engine parameters. The combustion chamber design can also be improved by replacing the 2-valve system with 4-valve system.

Using ceramics components such as piston pin, valves and blades in turbochargers has a significant impact on the pollutants emission. The turbo-compounded engine are found to be up to 18% better than the conventional engines.

On the other hand, the major pollutants from CI engine can be reduced as follows; Hydrocarbons emission control requires low-sac nozzle to improve the combustion. The nitrogen dioxides emission control is assisted by cooling the intake air before entering the engine resulting in retarded combustion. Finally, the particulate emissions control is associated with high injection pressure for a fine fuel atomization.

1.3 Purpose and Significance of the thesis

All mentioned methods of controlling the contaminations in a gas flow are not 100% efficient. So from our point of view, the ideal solution for the air pollution caused by the vehicles emissions is to eliminate the pollutant in the first place by utilizing the clean renewable energy sources to power the cars. Hence, we are designing a prototype of a vehicle that exploit the compressed natural air to push the pistons in the engine instead of combusting fuel. The purpose is to have a closer look on an engine with zero emission using the renewable energy with the minimum operating cost.

CHAPTER TWO

LITRATURE REVIEW

We are living in a very mobile society so light utility vehicles (LUV) like bikes and cars are becoming very popular means of independent transportation for short distances. Petrol and diesel which have been the main sources of fuel in the history of commuting, are becoming more expensive and impractical (especially from an environmental standpoint). Such factors are leading vehicle manufacturers to develop vehicles fueled by alternative energies. When at present level of technological development fuel-less flying (like birds) i.e., flying based on the use of bio-energy and air power in the atmosphere seems to be almost impossible for human beings then engineers are fascinated at least with the enormous power associated with the human friendly as well as tested source of energy (i.e., air) to make air-powered vehicles as one possible alternative. Engineers are guiding their true endeavors to utilize air as a fuel source to run the LUVs which will make future bicycles and light/little vehicles running with air power for every day schedule distances and the movement will be liberated from contamination and practical.

2.1 The Technology of Compressed Air Engine

Mankind has been making use of uncompressed air- power from centuries in different application viz., windmills, sailing, balloon car, hot air balloon flying and hang gliding etc. The use of compressed air for storing energy [3] is a method that is not only efficient and clean, but also economical and has been used since the 19th century to power mine locomotives, and was previously the basis of naval torpedo propulsion. In 1903, the Liquid Air Company located in London manufactured a number of compressed air and liquified air cars. The serious issue with compacted air vehicles was the absence of force delivered by the "motors" and the expense of packing the air. As of late a few organizations [1-5] have begun to create compacted air vehicles, albeit none has been delivered to the public up until now. Com-squeezed air tanks store power truly well however are missing on force thickness. They tie or beat batteries in the charge/re-charge proficiency and thoroughly execute them on life expectancy. Higher pressing factors are their huge issue of compacted air vehicles while productivity, cost, poisonous synthetics, and life expectancy are the enormous issues related with substance batteries. The rule of compacted air drive is to pres-surize the capacity tank and afterward interface it to something

exceptionally like a responding steam motor of the vehicle. Rather than blending fuel in with air and consuming it in the motor to drive cylinders with hot extending gases, packed air vehicles (CAV) utilize the development of compacted air to drive their cylinders. Accordingly, making the innovation liberated from troubles, both specialized and clinical, of utilizing alkali, petroleum, or carbon disulphide as the working liquid. Makers [5-9] case to have planned motor that is 90% proficient. The air is compacted at pressure around multiple times the rate the air is compressed into vehicle tires or bike. The tanks should be intended to wellbeing guidelines proper for a pressing factor vessel. The capacity tank might be made of steel, aluminum, carbon fiber, kevlar or different materials, or blends of the above mentioned. The fiber materials are significantly lighter than metals yet commonly more costly. Metal tanks can withstand an enormous number of pressing factor cycles, however should be checked for erosion occasionally. An organization has expressed to store air in tanks at 4,500 pounds for every square inch (around 30 MPa) and hold almost 3,200 cubic feet (around 90 cubic meters) of air. The tanks might be topped off at a help station outfitted with heat exchangers, or in a couple of hours at home or in parking areas, connecting the vehicle to an on-board blower.

2.2 Development of Compressed Air Engine

Jem Stansfield, an English inventor has been able to convert a regular scooter to a compressed air moped shown in Fig2.1 This has been finished by furnishing the bike with a packed air motor and air tank. Jem Stansfield made the bicycle by strong two high-pressure tanks onto the side of his Puch sulked The tanks are fundamentally scuba tanks. He utilizes the power from his home to fill the tanks



Fig 2.1: compressed air vehicle model

The force is then "put away" there, similar as a battery, prepared for use. The tanks utilized are carbon-fiber tanks of the sort utilized by firemen for oxygen. Yet at the same time, they're far less expensive than even the lead corrosive battery utilized in vehicle now. Obviously, the blower chips away at power, so that is not generally a spotless force source but rather re-energizing choices

around evening time or off pinnacle will upgrade the odds to utilize the force that would be squandered something else. The maximum velocity is around 18 mph, and it can just go 7 miles before the pneumatic force runs out and significantly more force could most likely be pulled by tweaking his setup. A little stuff on the finish of the air drill, associated with the chain of the bicycle would make a significantly more rich arrangement. A few organizations [1-9] are exploring and creating models, and others intend to offer air fueled vehicles, transports and trucks. The compacted air is put away in carbon-fiber tanks that are incorporated into the frame. As the air is delivered, the pressing factor drives cylinders that power the motor and move the vehicle, and the cylinders pack the air into a repository so the cycle proceeds. In the wake of making an unrest by delivering the world's least expensive vehicle Tata nano, India's biggest automaker (Tata Motors) is set to begin creating the world's first business air-controlled vehicle. The "Air Car" will utilize packed air, rather than the gas-and-oxygen blasts of inside ignition models, to push its motor's cylinders. Zero Pollution Motors (ZPM) (USA) [1] additionally hopes to create the world's first air-fueled vehicle for the United States by 2010. An earlier version of the car is noisy and slow, and a tiny bit cumbersome but then this vehicle will not be competing with a Ferrari or Rolls Royce and the manufacturers are also not seeking to develop a Formula One version of the vehicle. The aim of air powered vehicles is the urban motorist: delivery vehicles, taxi drivers, and people who just use their vehicles to nip out to the shops. The latest air car is said to have come on leaps and bounds from the early model. It is said to be much quieter, a top speed of 110 km/h (65 mph), and a range of around 200 km before you need to fill the tanks up with air.

2.3 Advantages of Compressed Air vehicles

In comparison to petrol or diesel powered vehicles “air powered vehicles” have the following advantages:

- Air, all alone, is non-combustible, plentiful, prudent, movable, storable and, above all, nonpolluting.
- Compressed air technology reduces the cost of vehicle production by about 20%, because there is no need to build a cooling system, fuel tank, spark plugs or silencers.
- High torque for minimum volume.
- The mechanical design of the engine is simple and robust.
- Low manufacture and maintenance costs as well as easy maintenance.

2.4 Drawback of compressed Air Engines

Disadvantages of compressed-air vehicles are less well known, since the vehicles are currently at the pre-production stage and have not been extensively tested by independent observers. Some bottlenecks of technology may be summarized as

- Compressed air vehicles probably will be less powerful than common vehicles of today. Which represents a peril to clients of packed air vehicles imparting the way to bigger, heavier and more inflexible vehicles
- At the point when the air is extended in the motor, it will chill off through adiabatic cooling and lose constrain in this way its capacity to take care of job at colder temperatures. It is hard to keep up or reestablish the air temperature by basically utilizing a heat exchanger with surrounding heat at the high stream rates utilized in a vehicle, subsequently the ideal isothermic energy limit of the tank won't be figured it out. Cold temperatures will likewise urge the motor to ice up.

CHAPTER THREE

METHODOLOGY, CALCULATIONS AND SIMULATION

The researches about the air compressed engines are rapidly progressing to provide a modern way to run the vehicles without the use of the combustion.

The air is drawn from the atmosphere and stored in tanks using a compressor. To power the vehicle, some air is released to the expansion chamber -equivalent to combustion chamber- where it pushes the piston downward generating the reciprocating motion which is then converted to rotary motion with the help of the crank shaft and connecting rod. To control the air flow from the tanks to the expansion chamber, a high speed shutter is used.

The same working principle is used in this project where the high speed shutter is replaced by 4 ways 5 ports solenoid valve and a pneumatic actuator takes the place of the cylinder and piston assembly.

3.1 The Pneumatic Setup

Figure 3.1 shows the final result of this project. As illustrated in the figure 3.2; through a manifold, a compressor quick release fitting, pressure gauge, safety relief valve, and ball valve are connected directly to the air cylinder. The air flows from the cylinder toward the 5-Ports 4-Ways solenoid valve through a pressure regulator to maintain a safe operating pressure in the solenoid valve and the pneumatic cylinder (140 PSI) and a ball valve to cut the air flow to the actuator.

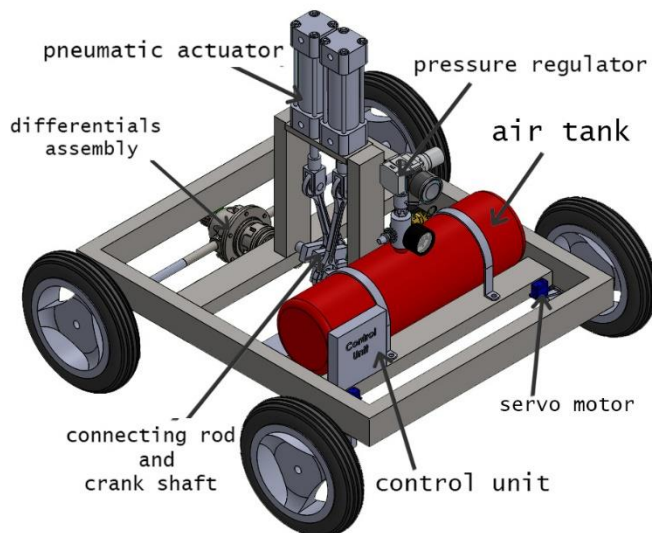


Fig 3.1: Final design of the project

The 5-Ports, 4-Ways solenoid valve is directly linked to the pneumatic cylinder and two flow control mufflers are associated with the solenoid valve to control the speed of the actuator's rod extending and retracting. The 5-Ports, 4-Ways solenoid valve is directly linked to the pneumatic cylinder and two flow control mufflers are associated with the solenoid valve to control the speed of the actuator's rod extending and retracting. The solenoid valve is connected to the control unit in order to control the operation of the pneumatic actuator. While the safety relief valve is used to evacuate the air cylinder.

The compressor quick release fitting is used to easily and quickly connect the compressor to the air cylinder for the refill.

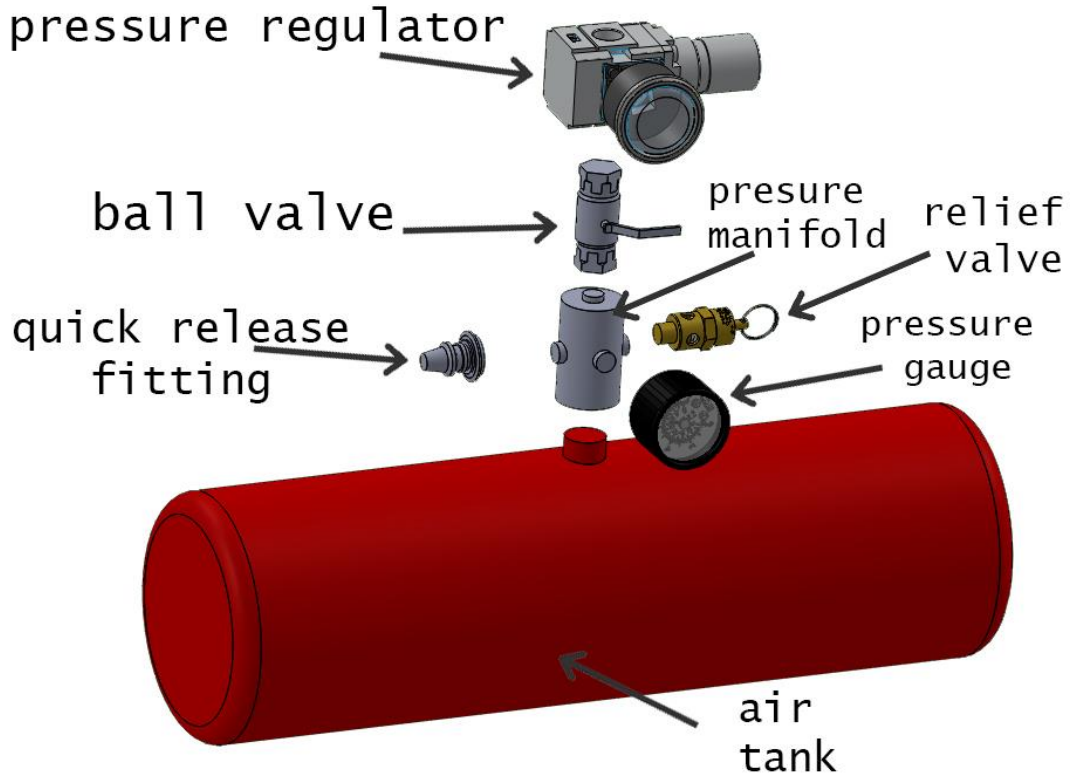


Fig 3.2: The pneumatic setup

3.2 The control unit

The control unit contains the receiver circuits to manage the operation of the 4 ways 5 ports solenoid valve and the steering system.

3.2.1 Controlling the 4 ways 5 ports solenoid valve

In order to control the solenoid valve, the following components are needed. 2 pieces of nrf24l01 2.4GHz wireless module, 9V toggle switch, two 10k Ω resistors, TIP120 Darlington Transistor, Rectifier diode (1N4001), 9 & 12V power sources, and two Arduino UNO R3 in addition to breadboards.

The following pictures show the different components needed in the circuits.

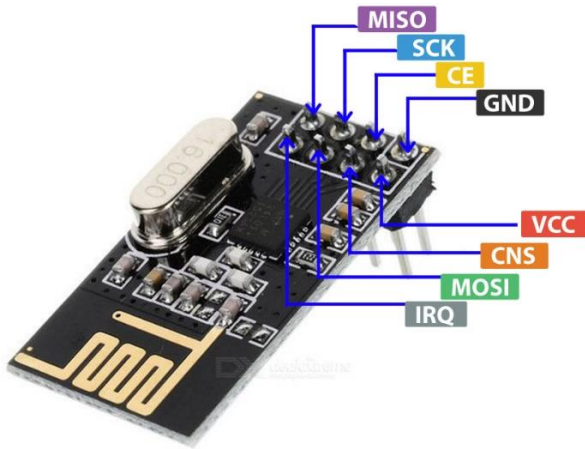


Fig 3.3: nrf24l01 wireless module pinout

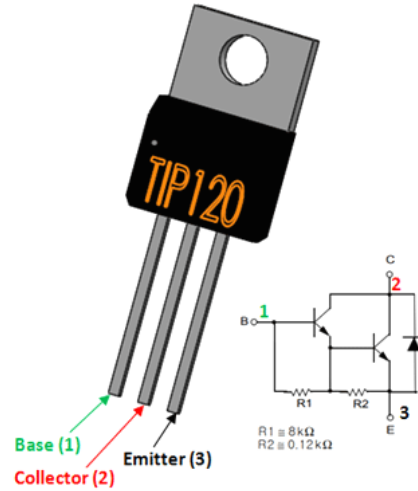


Fig 3.4: TIP120 Darlington transistor pinout

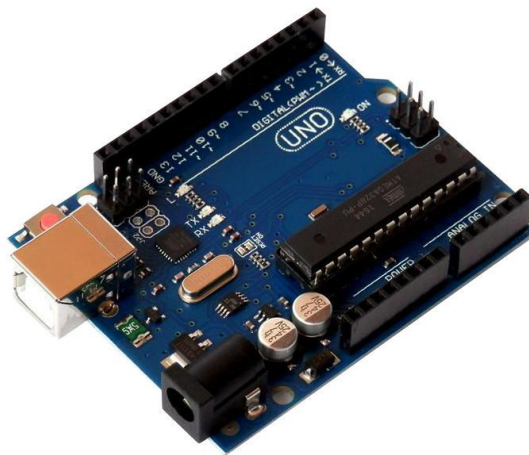


Fig 3.5: Arduino Uno R3

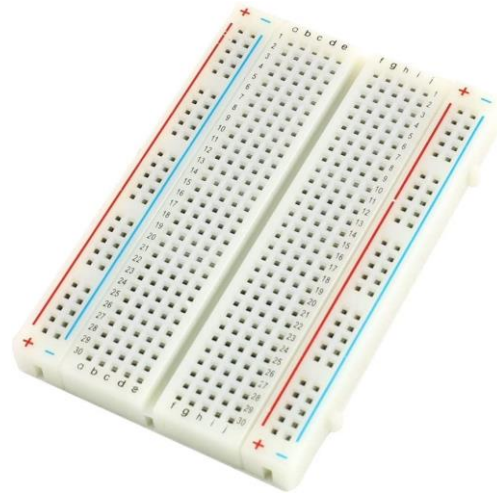


Fig 3.6: breadboard

To move the vehicle, the pneumatic actuator is remotely triggered using two Arduino circuits. The transmitter circuit initiates RF contact with the receiver circuit and sends it a message when the toggle switch is on. Wiring the nrf24l01 is the same in both transmitter and receiver circuits. However, the receiver Arduino circuit receives a signal performs an action which is to switch on the solenoid valve using the TIP120 Darlington transistor which allows 12V toward the solenoid once a signal is received from the transmitter circuit. Two pull-down resistor ($10k\Omega$) are used as a protection for the Arduino Unos from the high voltage. The Rectifier diode (1N4001) is required for the solenoid to prevent transient voltage from flowing through the system caused when a magnetic coil suddenly loses power once the solenoid is fired.

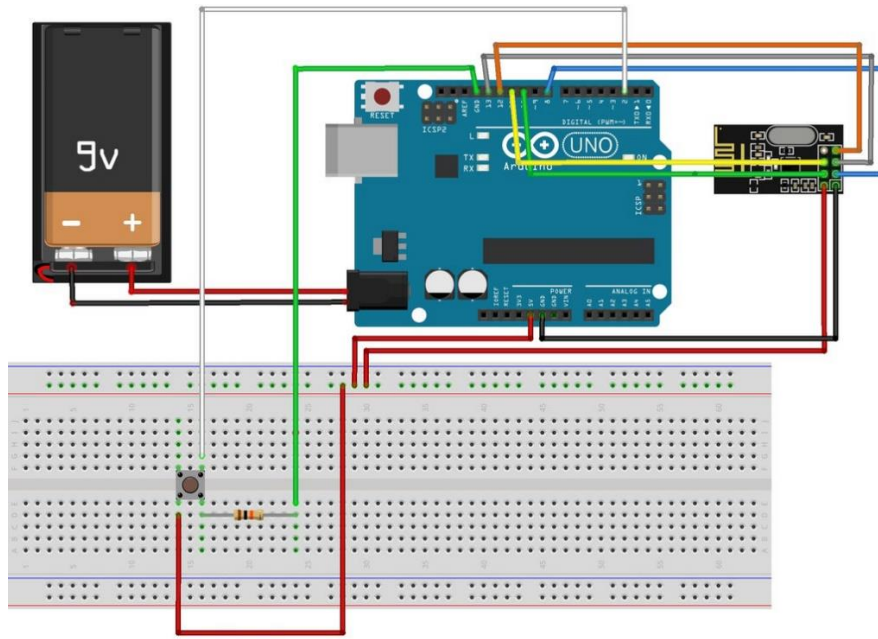


Fig 3.7: The transmitter circuit

The figure above shows the connection of the transmitter circuit used in controlling the 4 ways 5 ports solenoid valve. Here, 9V source is used to power the Arduino UNO R3 and one nrf24101 wireless module is used. The Arduino UNO R3 is programmed in such a way when the toggle switch is pushed, it sends signal to the nrf24101 wireless module which generates a radio frequency (RF) wave. The other Arduino UNO R3 in the receiver circuit is programmed so the nrf24101 wireless module works as a receiver. When the wireless module reads the RF wave, it sends signal to the TIP120 Darlington transistor allowing 12V to the solenoid. Figure 3.8 shows the circuit diagram of the transmitter circuit.

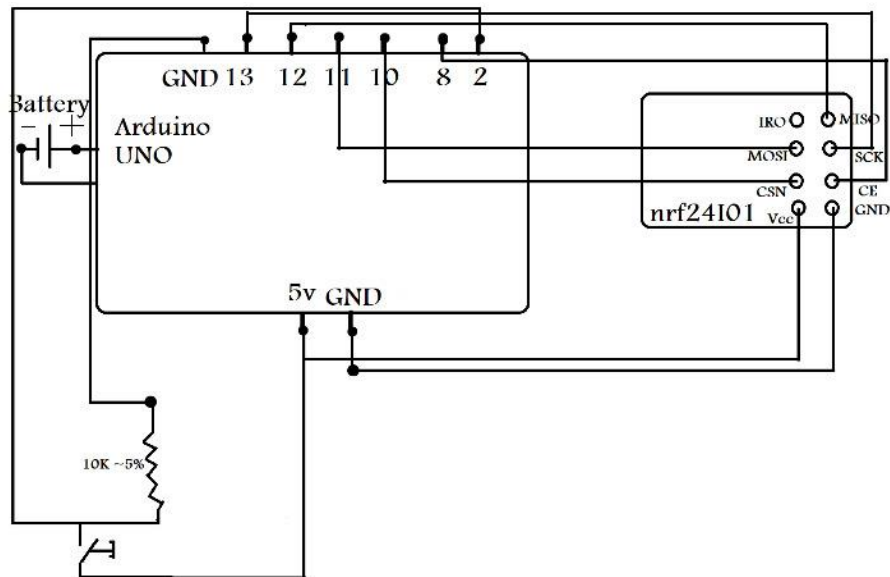


Fig 3.8: the transmitter circuit diagram

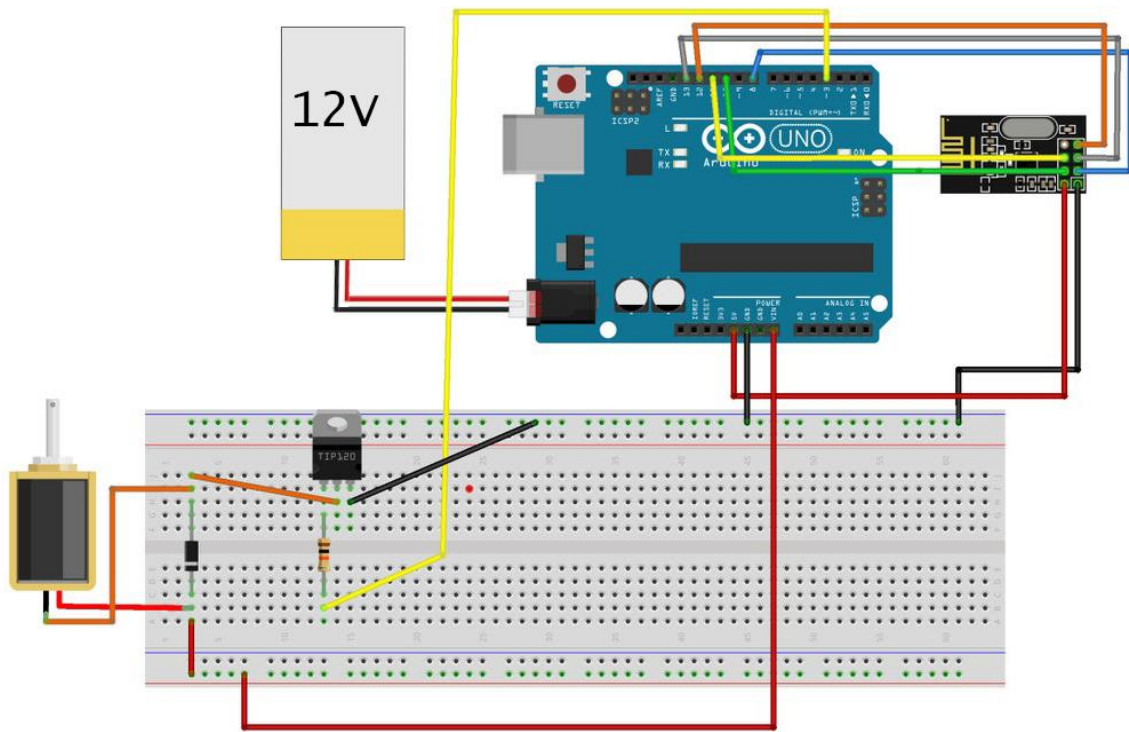


Fig 3.9: the receiver circuit

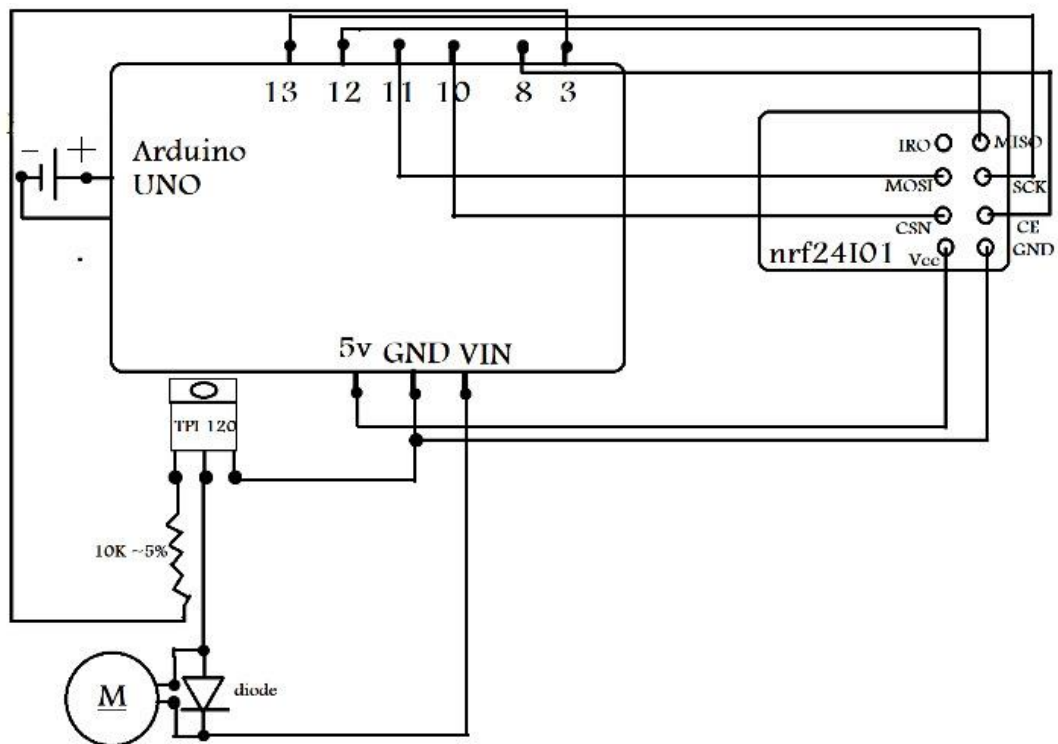


Fig 3.8: the receiver circuit diagram

```
sketch_feb23a $  
  
/*  
NRF24L01      Arduino  
CE           >   D8  
CSN          >   D10  
SCK          >   D13  
MO           >   D11  
MI           >   D12  
RO           >   Not used  
GND          >   GND  
VCC          >   5V  
*/  
#include <SPI.h>  
#include <RH_NRF24.h>  
const int button = 2;  
  
void setup()  
{  
  Serial.begin(9600);  
  if (!nrf24.init())  
    Serial.println("init failed");  
  // Defaults after init are 2.402 GHz (channel 2), 2Mbps, 0dBm  
  if (!nrf24.setChannel(125))  
    Serial.println("setChannel failed");  
  if (!nrf24.setRF(RH_NRF24::DataRate2Mbps, RH_NRF24::TransmitPower0dBm))  
    Serial.println("setRF failed");  
}  
void loop()  
{  
  if (digitalRead(button) == HIGH)  
  {  
    uint8_t data[] = "104";  
    nrf24.send(data, sizeof(data));  
  }  
  delay(50);  
}
```

Fig 3.9: The code used to program the Arduino UNO R3 in the transmitter circuit


```
sketch_feb23a $
/*
NRF24L01      Arduino
CE           >   D8
CSN          >  D10
SCK          >  D13
MO           >  D11
MI           >  D12
RO           >  Not used
GND          >  GND
VCC          >  5V
*/
#include <SPI.h>
#include <RH_NRF24.h>
const int FIRE = 3;
int timeOUT = 0;
RH_NRF24 nrf24;
void setup()
{
  pinMode(FIRE, OUTPUT);
  Serial.begin(9600);
  if (!nrf24.init())
    Serial.println("init failed");
  if (!nrf24.setChannel(125))
    Serial.println("setChannel failed");
  if (!nrf24.setRF(RH_NRF24::DataRate2Mbps, RH_NRF24::TransmitPower0dBm))
    Serial.println("setRF failed");
}
void loop()
{
  if (nrf24.available())
  {
    uint8_t buf[RH_NRF24_MAX_MESSAGE_LEN];
    uint8_t len = sizeof(buf);
    if (nrf24.recv(buf, &len)
        {
          Serial.print("got request: ");
          Serial.println((char*)buf);
          int sig = atoi((const char*) buf);
          if (sig == 104)
          {
            digitalWrite(FIRE, HIGH);
            timeOUT = 0;
            delay(150);
            digitalWrite(FIRE, LOW);
          }
        }
    else {
      if (timeOUT > 1000)
      {
        digitalWrite(FIRE, LOW);
        timeOUT++;
      }
    }
  }
}
```

Fig 3.9: The code used to program the Arduino UNO R3 in the receiver circuit

3.2.2 The steering system control

The steering mechanism rely on attaching the wheel shaft on a pivoted hinge. A servo motor with the help of a connecting rod pushes and pulls the hinge to change its angle to result in the vehicle's rotation.

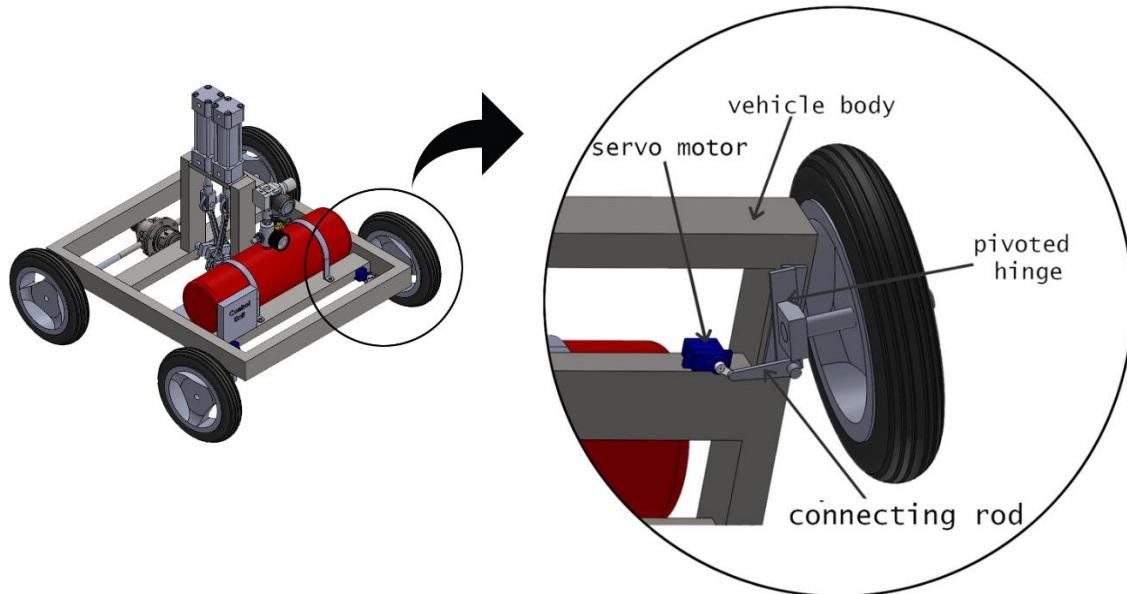
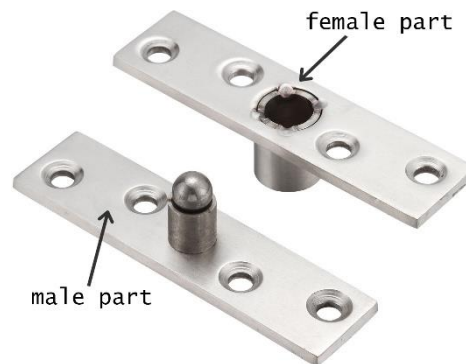


Fig 3.10: the steering mechanism

The pivoted hinge is made of stainless steel and it consists of two portions. The Female part which is mounted on the body of the vehicle. The second part is connected to the wheel shaft via the bearing. The male part is rotated by the operation of the servo motor.

The servo motor is a type of rotary actuators used for precise control of



angular position, velocity and acceleration. It generates high torque so it is capable of carrying upto 12 kg placed at 1 cm on its horn away from the axis of the shaft. Each of the front wheels has its own steering assembly. Both assemblies work simultaneously.

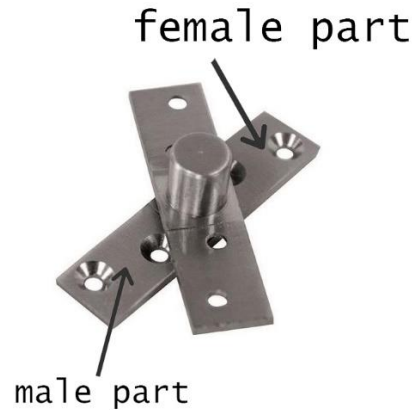


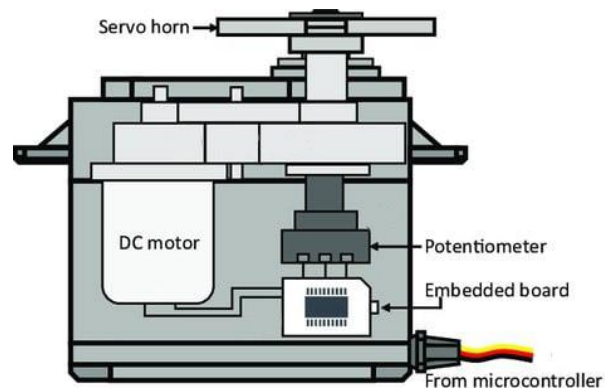
Fig 3.11: pivoted hinge

The horn of the servo motor is normally at 0 degrees when the car is moving forward. To make a right turn, the horn needs to be rotated 90 degrees counter clockwise. Similarly, it should be rotated 90 degrees in the clock wise direction so the vehicle makes a left turn.

For the steering system control, two nrf24l01 wireless modules, two servo motors, Arduino UNO R3, and 9V voltage source for the Arduino UNO R3 and the servomotor. In addition to a one axis joystick to determine the rotation direction. The lever of the joystick is attached to potentiometer. When the lever is displaced from its original position, a voltage difference is produced in the pins. The Arduino UNO R3 is programmed in such a way the servo motors sense this voltage difference then rotate at the same time at the same direction according to the orientation of the lever of the joystick.



Fig 3.12: Servo motor pinout



Fin 3.13: Servo motor construction



Fig 3.14: joystick

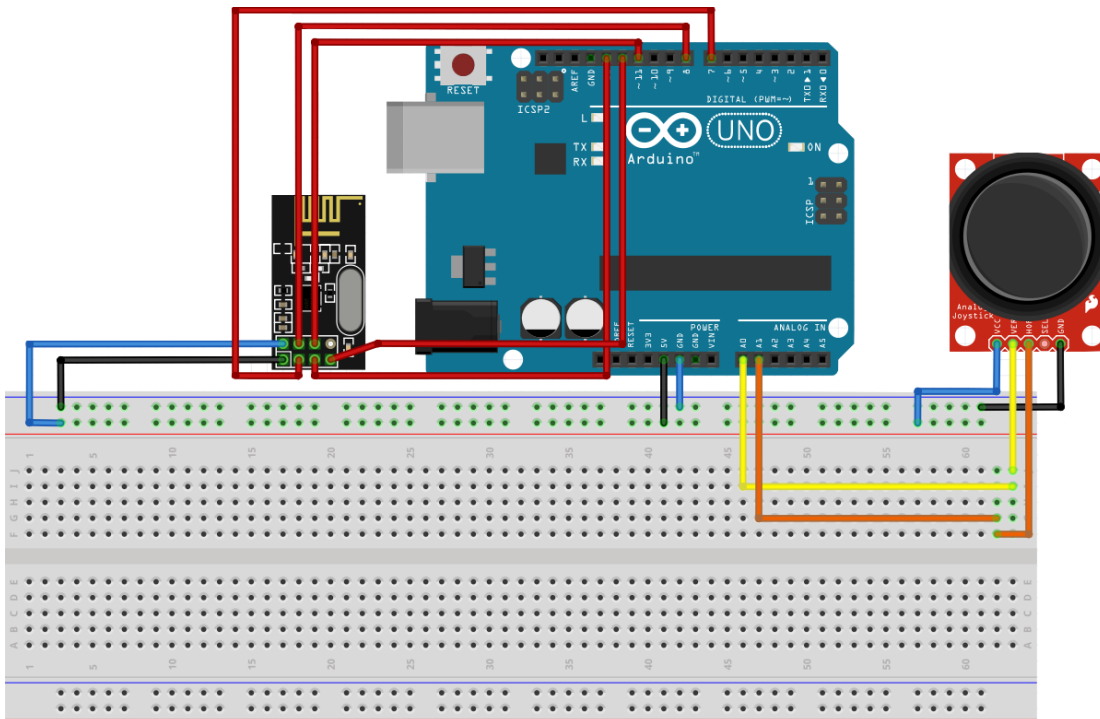


Fig 3.15: The transmitter circuit for the steering system

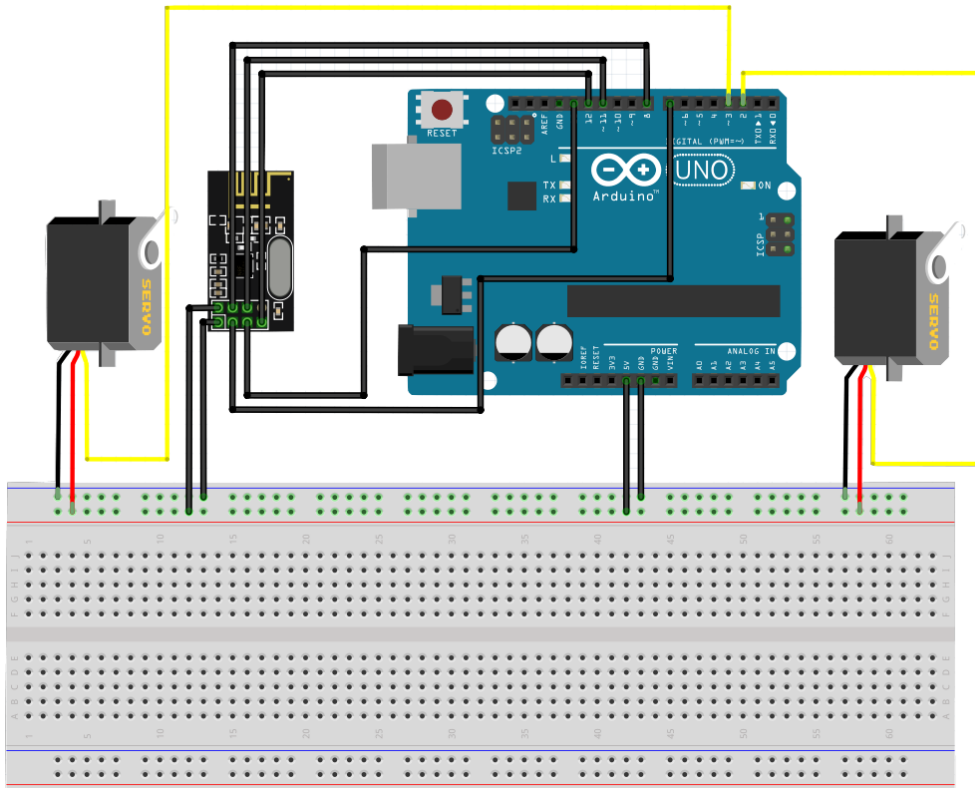


Fig 3.16: The receiver circuit for the steering system

```
sketch_feb23a $
#include <SPI.h>
#include <nRF24L01.h>
#include <RF24.h>

RF24 radio(7, 8);

const byte rxAddr[6] = "00001";

int sendingdata[6];

void setup()
{
  Serial.begin(9600);
  radio.begin();
  radio.setPALevel(RF24_PA_MAX);
  radio.setAutoAck(false);
  radio.setRetries(15, 15);
  radio.openWritingPipe(rxAddr);

  radio.stopListening();

  delay(50);
}

void loop()
{
  int in1 = analogRead(A0);
  int in2 = analogRead(A1);
  sendingdata[0]=in1;
  sendingdata[1]=in2;

  radio.write( sendingdata, sizeof(sendingdata) );
  Serial.print("RY =");
  Serial.println(sendingdata[0]);
  Serial.print("LY =");
  Serial.println(sendingdata[2]);
  delay(50);
}
```

Fig 3.17: The Arduino code for the transmitting circuit in the steering system

```
sketch_feb23a $
#include <SPI.h>
#include <RF24.h>
#include <Servo.h>

RF24 radio(7, 8);

const byte rxAddr[6] = "00001";
Servo yaw;
Servo thr;
int joystick[6];

void setup()
{
  for(int i = 2; i<=4; i++){
    pinMode(i,OUTPUT); }
  while (!Serial);
  Serial.begin(9600);
  radio.begin();
  radio.setPALevel(RF24_PA_MAX);
  radio.setAutoAck(false);
  radio.openReadingPipe(0, rxAddr);
  radio.startListening();
  thr.attach(2);
  yaw.attach(3);
  delay(50);
}

void loop(){
  if (radio.available())
  {
    bool done = false;
    while (!done)
    {
      // Fetching the data payload
      radio.read( joystick, sizeof(joystick) );
      done = true;

      int val0=map(joystick[0],0,1024,0,180);
      int val1=map(joystick[1],0,1024,0,180);
      thr.write(val0);
      yaw.write(val1);
      Serial.println(val0);
      Serial.println(val1);    } }
    else{
      Serial.println("Data not received");
    }
  }
  delay(50);
}
```

Fig 3.18: The Arduino code for the receiver circuit in the steering system

3.3 The crankshaft design

The crankshaft is an important part that converts the reciprocating motion of the piston into rotary motion through the connecting rod.

The crank shaft consist of three portions; crank pin, crank web and the shaft at the juncture of the crank web.

The connecting rod is attached to the crank pin which is connected to the shaft through the crank web. The shaft rotates in the bearings and transmits power to the differentials. Fig.1 illustrate the crank shaft layout. The crank shaft should have sufficient strength to withstand the bending and twisting moments to which it is subjected. In addition, it should have a sufficient rigidity to keep the lateral and angular deflection within permissible limits.

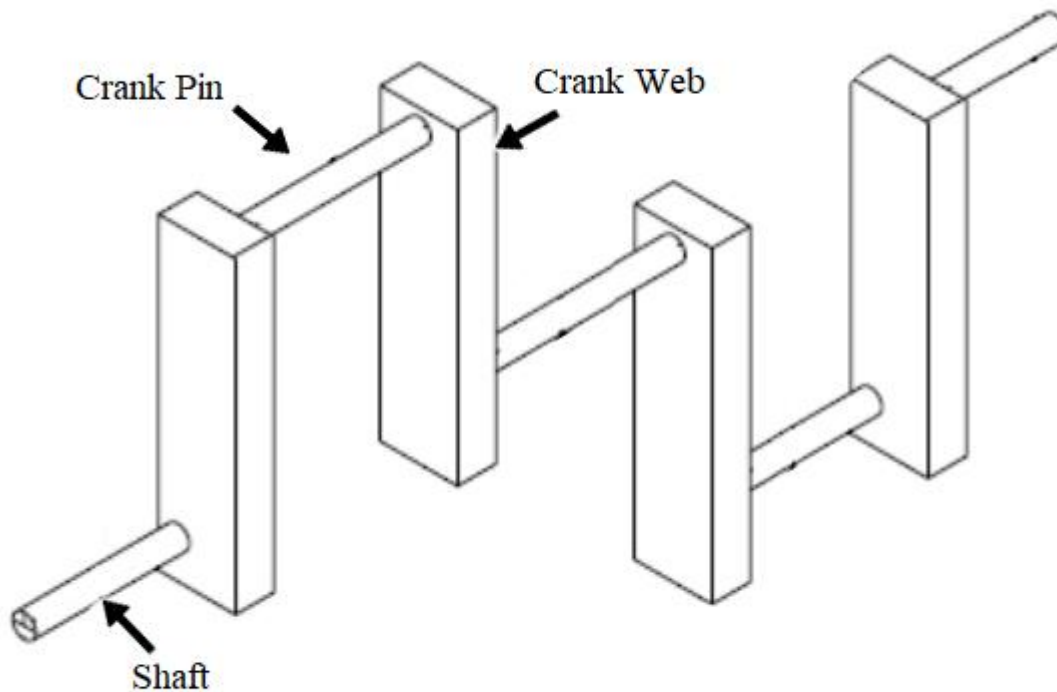


Fig. 1: The crank shaft layout

3.3.1 Crank shaft material

The crank shaft is considered to be manufactured from Cold Drawn AISI 1060 carbon steel with 0.6 wt.% carbon with a tensile strength and a yield strength of 620 MPa and 485 MPa respectively.

3.3.2 Crank shaft analysis and assumptions

To determine the dimensions of the crank shaft different portions, there are two cases of crank position to consider.

Case I: the crank at the top dead center position and subjected to maximum bending moment.

Case II: the crank is at an angle with the line of dead center positions and subjected to maximum torsional moment.

In both cases, the following assumptions are made:

- 1- Crank shaft is assumed to be a simply supported beam.
- 2- The factor of safety is 2 for shear and bending.
- 3- The maximum pressure in the cylinder is 140 psi
- 4- The cylinder bore and stroke are 40 mm and 80 mm.
- 5- The crank radius is 40 mm. ($0.5 \times stroke$)
- 6- The allowable bearing pressure at the crank pin bush is 10 MPa.

3.3.3 Analyzing the crank shaft at top dead center position

Fig. 2 shows the dimensions and the forces acting on the crank shaft when it is at top dead center position.

b : The distance between bearings a and 2

F_p : Force acting on the crank pin

$(R_1)_v$: The vertical component of the reaction force on bearing 1

$(R_2)_v$: The vertical component of the reaction force on bearing 2

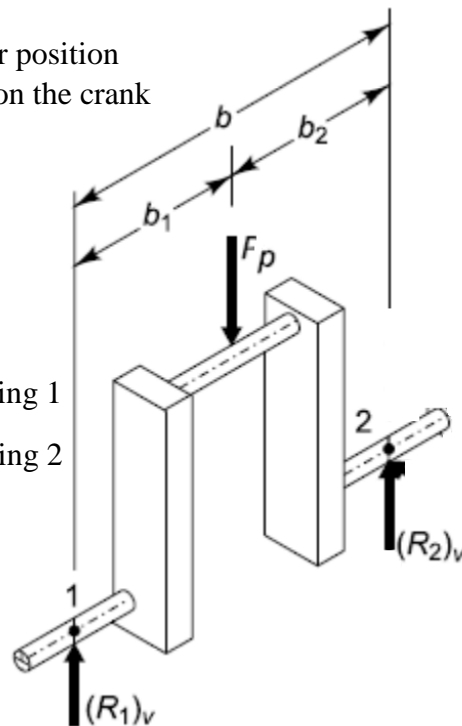


Fig. 2 : the forces acting on the crank shaft when it is in the top dead center

Bearing reactions

According to the manufacturer of the pneumatic actuator;

$$F_p = \text{pressure in pneumatic actuator}(\text{bar}) \times 0.126$$

$$F_p = 9.652 \times 0.126 = 1.216 \text{ KN} = 1216 \text{ N}$$

$$b(R_2)_v - b_1 F_p = 0 ; \text{ (The resultant moment about bearing 1)}$$

$$(R_2)_v = \frac{b_1}{b} F_p$$

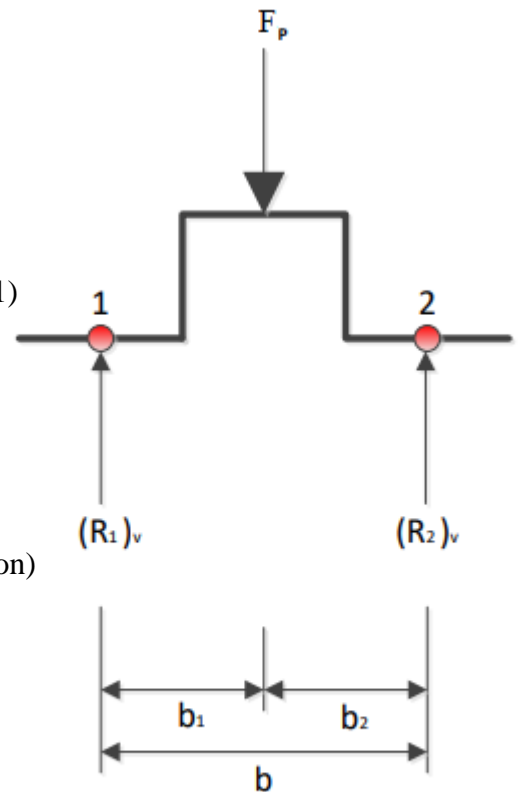
$$b_1 = 45 \text{ mm} , b_2 = 45 \text{ mm}$$

$$(R_2)_v = 0.5 \times F_p = 608 \text{ N}$$

$$(R_1)_v + (R_2)_v = F_p ; \text{ (Forces balance in the vertical direction)}$$

$$(R_1)_v = F_p - (R_2)_v$$

$$(R_1)_v = 1216 - 608 = 608 \text{ N}$$



Crank pin design

As shown in Fig. 3,

d_c : The crank pin diameter

l_c : The crank pin length

The bending moment at the central plane of the crank pin is given by;

$$(M_b)_c = (R_1)_v \times b_1 \dots (1)$$

$$\sigma_b = \frac{(M_b)_c \times y}{I}$$

$$(M_b)_c = \frac{\sigma_b \times I}{y} ; I = \frac{\pi d_c^4}{64} ; y = \frac{d_c}{2} ; \sigma_b = 0.5 \times \sigma_y$$

Where;

I : The second moment of inertia

σ_b : The allowable bending stress for the crank pin material

σ_y : The yield strength for the crank pin material

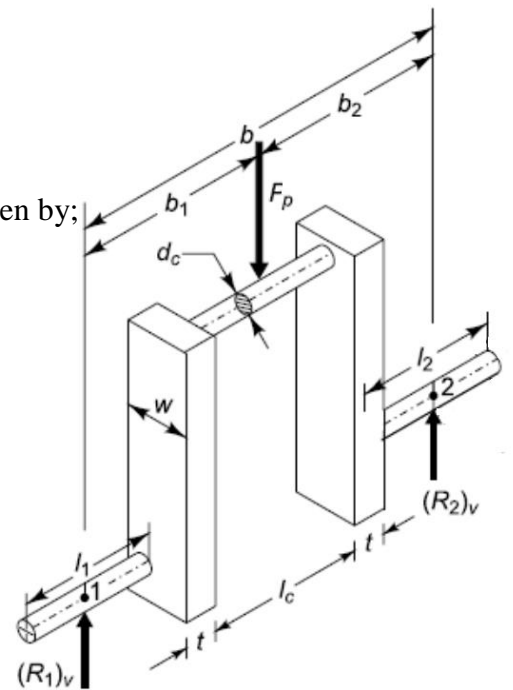


Fig.3 Crank Pin and Web

Substituting;

$$(M_b)_c = \frac{0.5 \times \sigma_y \times \pi \times (d_c^4 / 64)}{(d_c / 2)} \dots (2)$$

From equations (1) & (2)

$$d_c = \sqrt[3]{\frac{32 \times (R_1)_v \times b_1}{0.5 \times \pi \times \sigma_y}}$$

$$d_c = 10.48 \text{ mm}$$

$P_b = \frac{F_p}{l_c \times d_c}$; where P_b is the allowable bearing pressure at the crank pin bush

$$l_c = \frac{F_p}{d_c \times P_b} = \frac{1216}{10.48 \times 10} = 11.6 \text{ mm}$$

The crank pin diameter must be at least 10.48 mm while its maximum length is 11.6 mm to withstand the bending moment when the crank shaft in the top dead center position.

d_c is taken 15 mm and l_c is 10 mm

Crank web design

The minimum values of the crank web dimensions are calculated using empirical relations then checked for stresses.

$$t = 0.7 \times d_c = 0.7 \times 15 = 10.5 \text{ mm}$$

$$w = 1.14 \times d_c = 1.14 \times 15 = 17.1 \text{ mm}$$

t = the crank web thickness

w = the crank web width

The crank web thickness and width have to be at least 10.5 mm and 17.1 mm respectively.

t is taken 11 mm and w is 25 mm

As Fig. 3 shows, the central plane of the left-hand crank web is subjected to direct compressive stress and bending stress due to eccentricity of $(R_1)_v$.

The direct compressive stress, $\sigma_c = \frac{(R_1)_v}{w \times t} = \frac{608}{25 \times 11} = 2.211 \text{ MPa}$

The bending stress, $\sigma_b = \frac{M_b \times y}{I}$; $y = \frac{t}{2}$; $I = \frac{w \times t^3}{12}$; $M_b = (R_1)_v \times (b_1 - \frac{l_c}{2} - \frac{t}{2})$

$$\sigma_b = \frac{(R_1)_v \times (b_1 - \frac{l_c}{2} - \frac{t}{2}) \times \frac{t}{2}}{\frac{w \times t^3}{12}} = \frac{608 \times (45 - \frac{10}{2} - \frac{11}{2}) \times \frac{11}{2}}{\frac{25 \times 11^3}{12}} = 41.60 \text{ MPa}$$

The total compressive stress $\sigma_{total} = \sigma_b + \sigma_c = 41.60 + 2.211 = 43.811 \text{ MPa}$

For a safe design, the total compressive stress shouldn't exceed the allowable bending stress for the web material, $\sigma_{b,allowable}$

$$\sigma_{b,allowable} = 0.5 \times \sigma_y = 242.5 \text{ MPa}$$

The design is secure when the crank shaft is the top dead center position.

The right-hand crank web is made identical to the left-hand web for a balanced crank shaft.

3.3.4 Analyzing the crank shaft when it is subjected to maximum torsional moment

F_p : Force acting on piston due to gas pressure

F_q : Thrust on connecting rod

F_t : Tangential component of force on crank pin

F_r : Radial component of force on crank pin

θ : Angle of inclination of crank with the line of dead centers

ϕ : Angle of inclination of connecting rod with the line of dead centers

L : Connecting rod length

r : Crank radius

Components of force on crank pin

$$\sin \phi = \frac{\sin \theta}{(L/r)} = \frac{\sin 30}{(100/30)}$$

$$\phi = 14.5^\circ$$

$$F_q = \frac{F_p}{\cos \phi} = 1256 \text{ N}$$

$$F_t = F_q \sin(\theta + \phi) = 880.34 \text{ N}$$

$$F_r = F_q \cos(\theta + \phi) = 896 \text{ N}$$

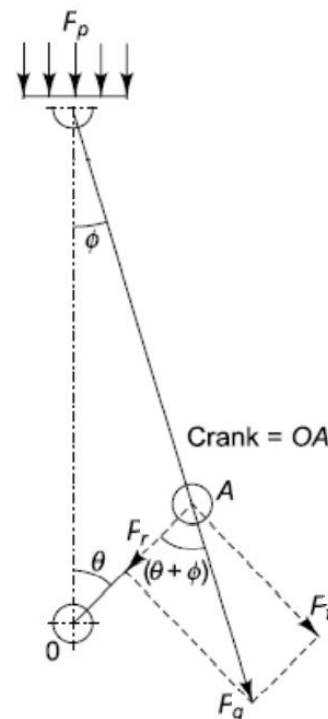


Fig. 4: The crankshaft at angle of maximum torque

Bearing reactions

Due to the tangential component F_t there are reactions $(R_2)_h$ and $(R_1)_h$. Similarly, the reactions $(R_1)_v$ and $(R_2)_v$ are due to the radial component of F_q at the crank pin.

From the moment of horizontal forces about bearing 1;

$$F_t \times b_1 = (R_2)_h \times b ;$$

$$(R_2)_h = \frac{F_t \times b_1}{b} = 440.17 \text{ N}$$

From the moment of horizontal forces about bearing 2;

$$F_t \times b_2 = (R_1)_h \times b$$

$$(R_1)_h = \frac{F_t \times b_2}{b} = 440.17 \text{ N}$$

From the moment of vertical forces about bearing 1;

$$F_r \times b_1 = (R_2)_v \times b$$

$$(R_2)_v = \frac{F_r \times b_1}{b} = 448 \text{ N}$$

From the moment of vertical forces about bearing 2;

$$F_r \times b_2 = (R_1)_v \times b$$

$$(R_1)_v = \frac{F_r \times b_2}{b} = 448 \text{ N}$$

The resultant reaction forces at the bearing are

$$R_1 = \sqrt{[(R_1)_h]^2 + [(R_1)_v]^2} = 628.055 \text{ N}$$

$$R_2 = \sqrt{[(R_2)_h]^2 + [(R_2)_v]^2} = 628.055 \text{ N}$$

Crank pin design

Due to the components of the reaction force at bearing 1, the central plan of the crank pin is associated to bending moment M_b and torsional moment M_t .

$$M_b = (R_1)_v \times b_1$$

$$M_t = (R_1)_h \times r$$

The crank pin diameter (d_c) is calculated by the formula $d_c^3 = \frac{16}{\pi \times \tau} \sqrt{(M_b)^2 + (M_t)^2}$

$\tau = 0.5 \times \text{the tensile strength of the crank pin material}$

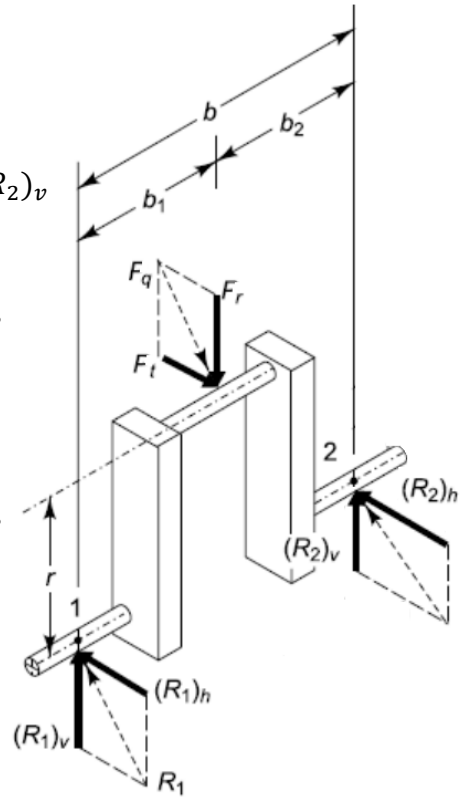


Fig. 5: crank shaft at angle of maximum torque

Where (τ) is the allowable shear stress.

$$\tau = 0.5 \times 620 = 310 \text{ MPa}$$

$$\begin{aligned} d_c^3 &= \frac{16}{\pi \times \tau} \sqrt{[(R_1)_v \times b_1]^2 + [(R_1)_h \times r]^2} \\ &= \frac{16}{\pi \times 310} \sqrt{[448 \times 45]^2 + [440.17 \times 40]^2} = 440 \end{aligned}$$

$$d_c = 7.6 \text{ mm}$$

The crank pin diameter should be at least 7.6 mm to withstand the maximum torque. The pre-determined crank pin diameter (15 mm) serves a secure design.

$$l_c = \frac{F_q}{d_c \times P_b} = \frac{1256}{7.6 \times 10} = 16.53 \text{ mm}$$

The maximum value of the crank pin length shouldn't exceed 16.53 mm to serve a secure design when the crank pin is subjected to maximum torque. The crankpin length is take as 10 mm to be within the secure span.

Design of shaft at the juncture of right-hand crank web

d_s : the diameter of the shaft at the juncture of right – hand crank web

In addition to the bending moment in both vertical and horizontal directions due to the forces in the vertical and horizontal planes, the shaft is affected by a torsional moment due to the tangential component of F_q .

$(M_b)_v$: The bending moment in the vertical direction due to $(R_1)_v$ and F_r

$(M_b)_h$: The bending moment in the horizontal direction due to $(R_1)_h$ and F_t

M_t : The torsional moment due to F_t

$$(M_b)_v = (R_1)_v \left[b_1 + \frac{l_c}{2} + \frac{t}{2} \right] - F_r \left[\frac{l_c}{2} + \frac{t}{2} \right] = 15456 \text{ N.mm}$$

$$(M_b)_h = (R_1)_h \left[b_1 + \frac{l_c}{2} + \frac{t}{2} \right] - F_t \left[\frac{l_c}{2} + \frac{t}{2} \right] = 15185.9 \text{ N.mm}$$

$$M_b = \sqrt{[(M_b)_v]^2 + [(M_b)_h]^2} = 21668 \text{ N.mm}$$

$$M_t = F_t \times r = 880.34 \times 40 = 35213.6 \text{ N.mm}$$

$$d_s^3 = \frac{16}{\pi \times \tau} \sqrt{(M_b)^2 + (M_t)^2} = 380$$

$$d_s = 7.25 \text{ mm (The minimum value)}$$

The diameter of the shaft at the juncture of right-hand crank web is considered as 15 mm

Crank web design

The right-hand crank web is associated to a bending stress in both vertical and horizontal planes, direct compressive stress and a torsional stress.

The bending moment due to radial component;

$$(M_b)_r = (R_2)_v \left[b_2 - \frac{l_c}{2} - \frac{t}{2} \right] \dots (3)$$

$$(M_b)_r = (\sigma_b)_r \times Z; \quad Z = \frac{w \times t^2}{6}$$

$$(M_b)_r = (\sigma_b)_r \times \frac{w \times t^2}{6} \dots (4)$$

Using equations 3 and 4, the bending stress due to radial component $(\sigma_b)_r$ is

$$(\sigma_b)_r = \frac{6 \times (R_2)_v \left[b_2 - \frac{l_c}{2} - \frac{t}{2} \right]}{w \times t^2} = 30.66 \text{ MPa}$$

The bending moment due to tangential component at the juncture of the crank web shaft;

$$(M_b)_t = F_t \left[r - \frac{d_s}{2} \right] \dots (5)$$

$$(M_b)_t = (\sigma_b)_t \times Z; \quad Z = \frac{w \times t^2}{6}$$

$$(M_b)_t = (\sigma_b)_t \times \frac{w \times t^2}{6} \dots (6)$$

From equations 5 and 6, the bending stress due to tangential component $(\sigma_b)_t$ is

$$(\sigma_b)_t = \frac{6 \times F_t \left[r - \frac{d_s}{2} \right]}{w \times t^2} = 56.75 \text{ MPa}$$

The direct compressive stress due to radial component is

$$(\sigma_c)_d = \frac{F_r}{2 \times w \times t} = 1.63 \text{ MPa}$$

The total compressive stress σ_c is obtained by

$$\sigma_c = (\sigma_b)_r + (\sigma_b)_t + (\sigma_c)_d = 89.04 \text{ MPa}$$

The torsional moment on the arm is

$$M_t = (R_1)_h \left[b_1 + \frac{l_c}{2} \right] - P_t \left[\frac{l_c}{2} \right] = (R_2)_h \left[b_2 - \frac{l_c}{2} \right] = 17386.715 \text{ N.mm}$$

$$\tau = \frac{M_t}{Z_p} = \frac{4.5 \times M_t}{w \times t^2} = 25.86 \text{ N/mm}^2$$

$$Z_p = \frac{w \times t^2}{4.5} = \text{polar section modulus}$$

The maximum compressive stress is given by

$$(\sigma_c)_{max} = \frac{\sigma_c}{2} + \frac{1}{2}\sqrt{(\sigma_c)^2 + 4 \times \tau^2} = 96 \text{ MPa} < 310 \text{ MPa}$$

Since the maximum compressive stress is less than the allowable compressive stress, the design is safe.

The thickness and width of the left-hand crank web are made identical to that of the right-hand crank web from balancing consideration.

Crankshaft dimensions

1. Crank radius 40 mm
2. Crank pin diameter 15 mm
3. Crank pin length 10 mm
4. Crank web thickness 11 mm
5. Crank web width 25 mm
6. The shaft diameter 15 mm

3.3.5 Testing the crank shaft design using finite element method

To confirm the safety of the crank shaft, the dimensions resulted from the analytical solution were examined using the finite element method in the SolidWorks 2018 software. An obstacle was faced. Which is not finding the AISI 1060 steel in the SolidWorks library. So AISI 1045 steel was used. If the design is safe using the 1045 steel, it is definitely safe using the 1060. Table 1 shows the properties of the material used in this study.

Material Properties	
Name	: AISI 1045 Steel, cold drawn
Model type	: Linear Elastic Isotropic
Default failure criterion	: Max von Mises Stress
Yield strength	: 5.3e+08 N/m ²
Tensile strength	: 6.25e+08 N/m ²
Elastic modulus	: 2.05e+11 N/m ²
Poisson's ratio	: 0.29
Mass density	: 7850 kg/m ³
Shear modulus	: 8e+10 N/m ²
Thermal expansion coefficient	: 1.15e-05 /Kelvin

Table1: the mechanical properties of AISI 1045.

Firstly, a model of the crank shaft was drawn in the SolidWorks. Then, the geometry is separated to number of small elements is such a process called generating the mesh as shown in figure 6. Next is defining the boundary conditions. In this study, the shaft relying on the bearing is set to be fixed while the force from the piston is applied normally on the crank pin.

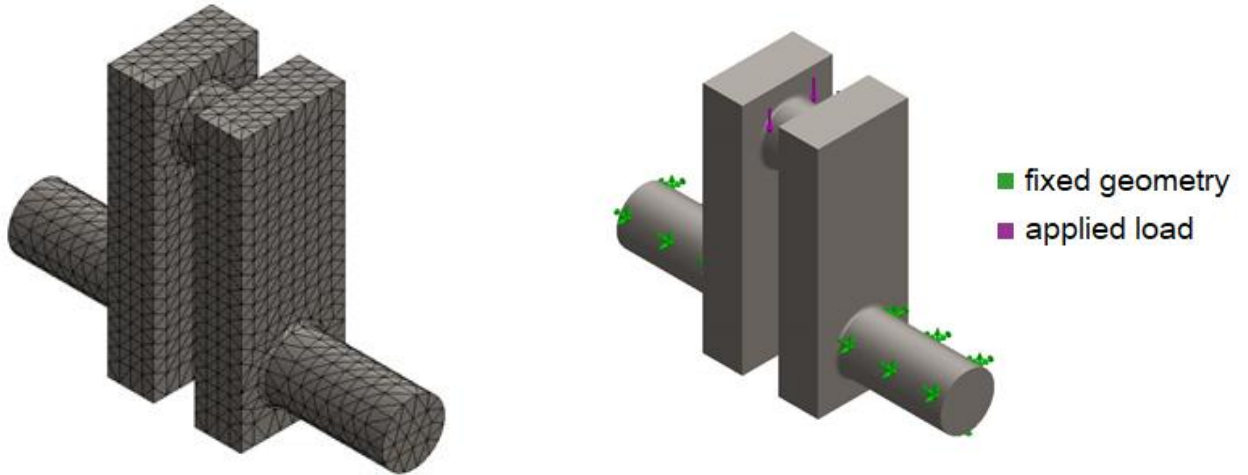
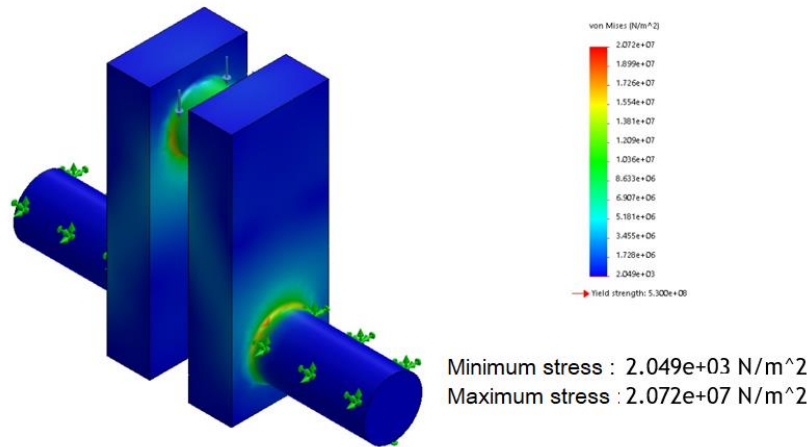


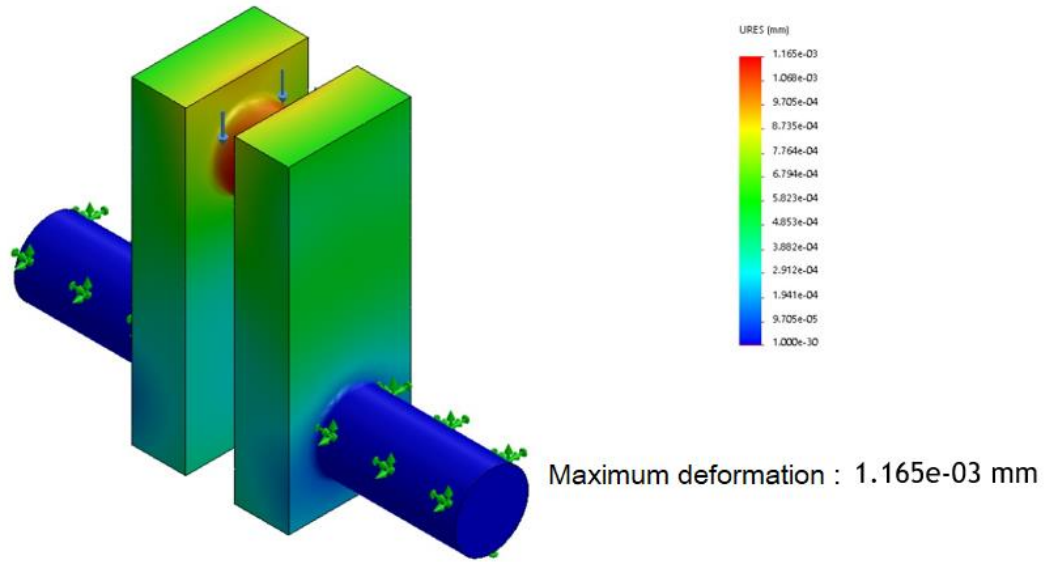
Figure 6: Crank shaft geometry after mesh Figure 7: Boundary conditions of the simulation

Figures 8, 9 and 10 show the result for the stresses on different portions of the crank shaft, the crank shaft deformation and the strain respectively. The maximum stress is ways less than the allowable stress for the material. $1.165e-03$ mm is very small for the deformation. The maximum strain is $6.775e-5$. Since this value is very small the geometry will keep its shape.



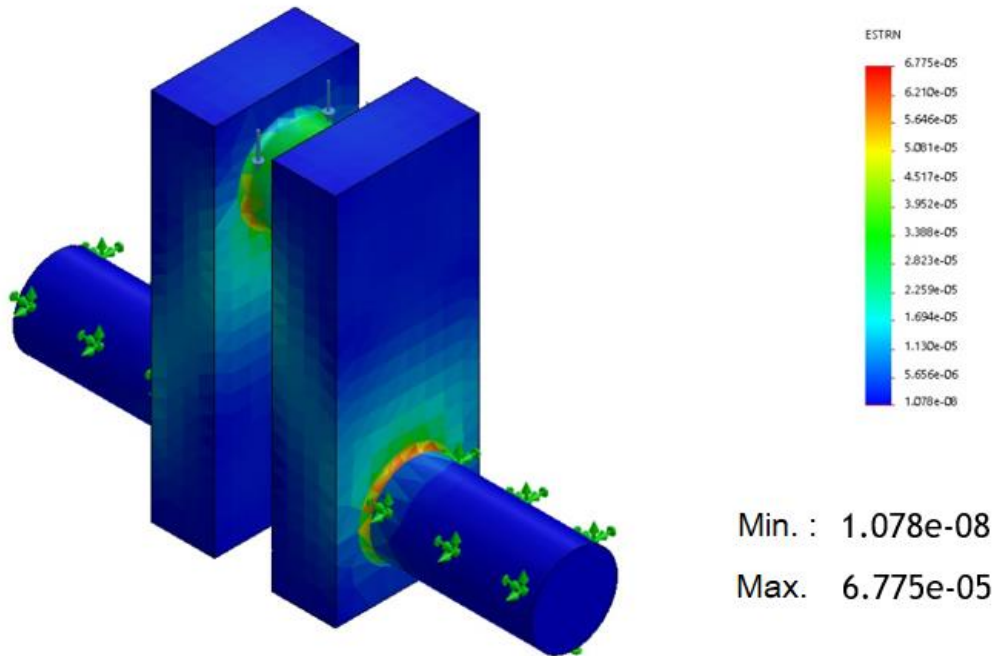
crank shaft- Stress result

Figure 8: the stresses acting on the crankshaft



crank shaft-Deformation result

Figure 9: The deformation of the crankshaft



crank shaft-Strain result

Figure 10: The strain of the crankshaft.

3.4 Connecting rod design

The connecting rod is that part on the engine responsible of transmitting the force from the piston into the crankpin. It is usually made in the shape of I-beam which consists, as shown in figure 1, of two horizontal planes 'flanges' connected with a vertical component 'web'.

The connecting rod, shown in figure 2, has a solid eye from one end in order to connect it with the piston, and a bolted eye from the end connected with the crankpin.

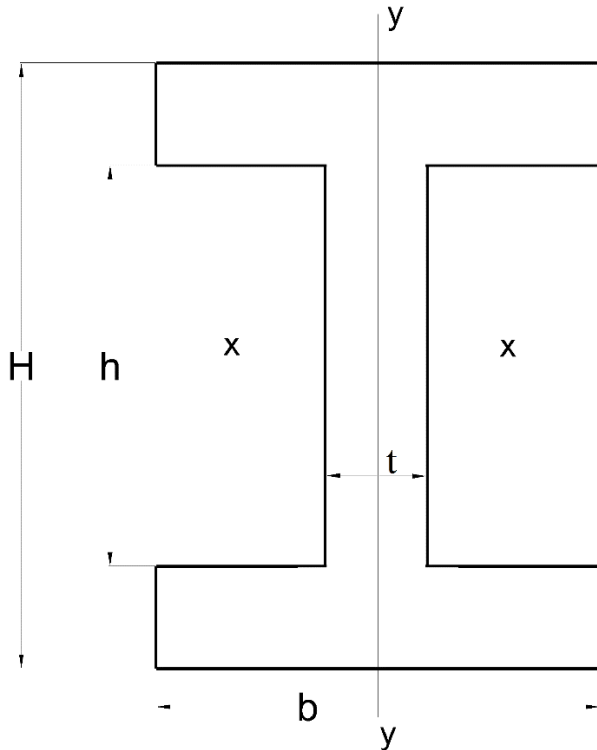


Fig 1: The cross-section of a connecting rod

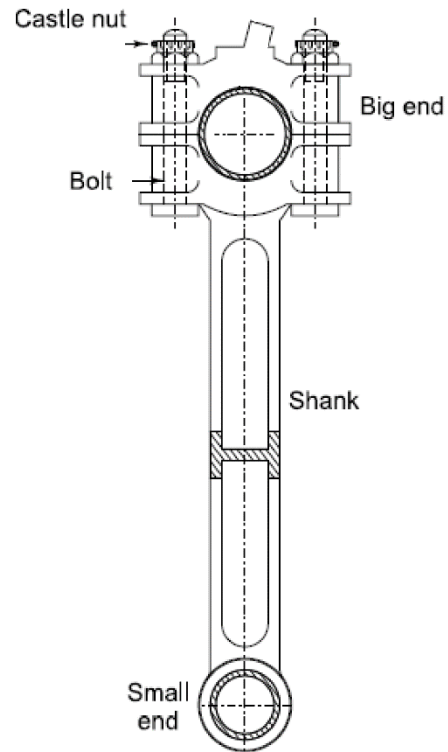


Fig 2: Connecting rod

3.4.1 Connecting rod material

The connecting rods is considered to be made of cold drawn medium carbon steel AISI 1045 steel with a yield strength of 310 MPa, and an ultimate tensile strength of 565 MPa.

3.4.2 Connecting rod dimensions

The connecting rod length

The connecting rods length is usually between 1.4 and 2.2 times the stroke, means it should lie in the range of 112 mm to 176 mm for this prototype. Here, the length of the connecting rod is arbitrary taken as 145 mm.

The shank thickness, height and breadth

The height and breadth of the I-section are functions of its thickness. The thickness is determined to resist the buckling as a result of the force.

It is found that the moment of inertia about the YY-axis needs to be 4 times the moment of inertia about XX-axis since the I-beam tends to buckle about that axis before buckling about the YY-axis. The typical magnitudes of the height and breadth at the middle of the crank shaft that satisfy this statement, as shown in figure 3, are $5t$ and $4t$ respectively. Where t is the thickness. The breadth is constant across the length while the height at the big end can be upto 1.25 times the height at the middle plane.

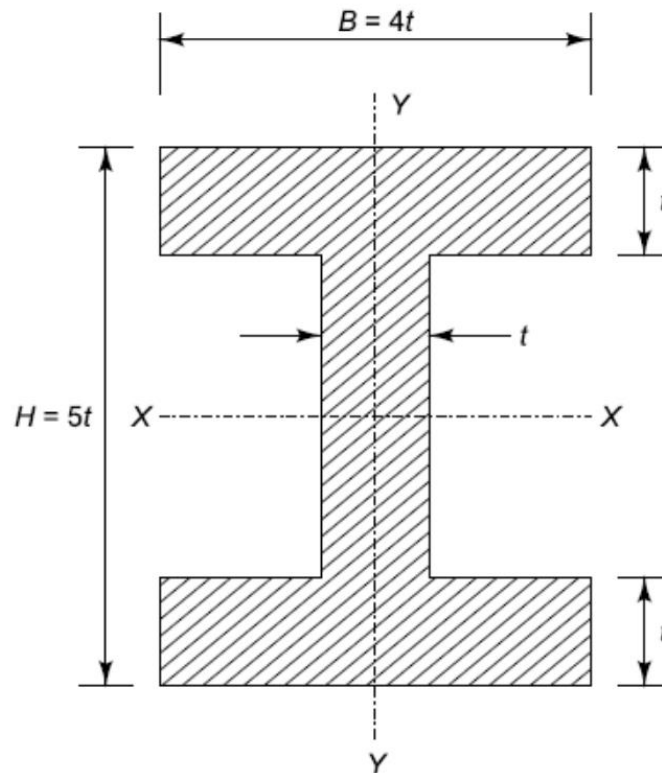


Fig 3: typical dimensions of the connecting rod at the middle

Determining the thickness of the I-beam starts by calculating the critical buckling load considering the factor of safety

$$F_{cr} = n \times F_c$$

F_{cr} ; The critical buckling load

F_c : The force acting on the connecting rod from the piston.

n : The factor of safety (n = 3)

$$F_{cr} = 3 \times 1216 = 3648 \text{ N}$$

Then, using Euler's formula in XX-direction.

$$F_{cr} = \frac{K\pi^2 EI_{xx}}{L^2}$$

Where;

K : constant depends on the ends condition. For the connecting rod, both ends are hinged (K=1)

L ; Connecting rod length

I_{xx} ; Moment of inertia

E ; modulus of elasticity (200 GPa)

Referring to figure 3;

$$I_{xx} = \frac{(4t)(5t)^3}{12} - \frac{(4t-t)(5t-2t)^3}{12} = \frac{419t^4}{12}$$

$$3648 = \frac{\pi^2 \times 200 \times 10^3 \left(\frac{419t^4}{12} \right)}{145^2}$$

By solving this equation, the minimum thickness to withstand the buckling result as 1.027 mm.

So, the dimensions of the connecting rod at the middle are;

The thickness (t) = 2 mm

The breadth (B) = 8 mm

The height (H) = 10 mm, the height at the big end is 12 mm

3.4.3 The ends of the connecting rod

The bearings of the connecting rod

The bearing at the small end of the connecting rod is usually a solid one-piece phosphor bronze bush of 3 mm thickness. The inner diameter of the bush equals the diameter of the piston pin diameter which is 12 mm.

The length of the bush is determined using the l/d ratio. Where l is the length and d is the diameter of the bush.

$$l/d = 2$$

$$l = 2d = 22 \text{ mm}$$

The big end of the connecting rod is mounted on the crank pin. The bearing here is a lined bush split into two halves with a 0.05 mm bearing crush. The inner diameter of the bush is the diameter of the crank pin which is 15 mm. the length of the bearing can be calculated using the following formula.

$$F_c = d \times l \times P_b$$

Where;

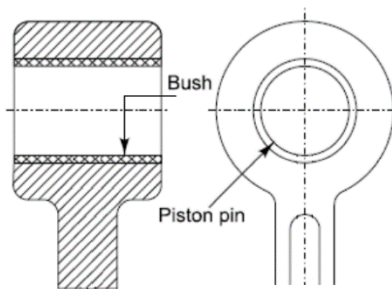
F_c : The force acting on the connecting rod

d : The inner diameter of the bush

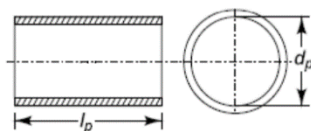
l : The length of the bush

P_b : The allowable bearing pressure

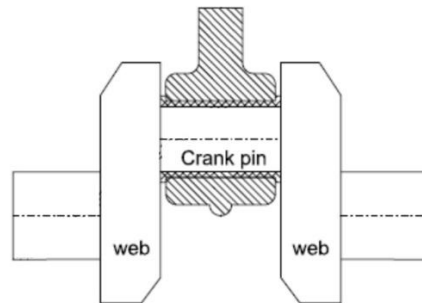
$$l = \frac{F_c}{d \times P_b} = \frac{1216}{15 \times 10} = 8.10 \text{ mm} , \text{ the bush length is taken as } 10 \text{ mm.}$$



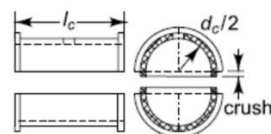
(a) Small end of connecting rod



(b) Bearing bush



(a) Big end of connecting rod



(b) Bearing bush

Fig 4: The small end of the connecting rod Fig 5: The big end of the connecting rod

The bolts and cap of the big end

The bolts of the big end cap are affected only by the inertia force of the reciprocating masses at the top dead center.

The inertia force is given by;

$$F_i = m_r \omega^2 r \left(\cos(\theta) + \frac{\cos(2\theta)}{n_1} \right)$$

F_i : The inertia force

m_r : The mass of the reciprocating parts (arbitrary 2 kg)

ω : The angular velocity of the crank shaft

r : The crank radius

θ : Angle of inclination of crank with the line of dead centers

n_1 : Ratio of length of the connecting rod to the crank radius

At the top dead center, θ is zero.

$$F_i = m_r \omega^2 r \left(1 + \frac{1}{n_1} \right) = 2 \times \left(\frac{2 \times \pi \times 60}{60} \right)^2 \times 40 \times \left(1 + \frac{40}{145} \right) = 4025.5 \text{ N}$$

The two bolts are subjected by equally distributed tensile force. Therefore, the inertia force affects the bolts is

$$F_i = 2 \left(\frac{\pi d_{core}^2}{4} \right) \sigma_c$$

d_{core} : The core diameter of the bolts

σ_c : The permissible tensile stress for bolts material

The bolts are made of alloy steel with an ultimate tensile strength of 720 MPa

$$\sigma_c = \frac{\text{ultimate tensile strength}}{\text{factor of safety}} = \frac{720}{2} = 360 \text{ MPa}$$

$$d_{core} = \sqrt{\frac{4F_i}{2\pi\sigma_c}} = \sqrt{\frac{4 \times 4025.5}{2 \times 3.14 \times 360}} = 2.67 \text{ mm}$$

The nominal diameter of the bolts $d_{nominal} = \frac{d_{core}}{0.8} = 3.3375 \text{ mm}$

Hence, M5X0.8 bolt is used.

The cap is also subjected to the inertia force. The cap is considered as a beam freely supported at the bolts centers and loaded in such a way that the bending moment is $\frac{wl}{6}$

$$M_b = \frac{P_i l}{6}$$

M_b : The bending moment

l : The distance between bolts centers

$l = \text{crankpin dia} + 2 \times \text{bush thickness} + \text{nominal diameter of bolts} + 6 \text{ mm clearance}$

$$l = 15 + 2 \times 3 + 5 + 6 = 32 \text{ mm}$$

$$M_b = \frac{4025.5 \times 32}{6} = 21469.33 \text{ N.mm}$$

$$M_b = \frac{I \sigma_b}{y}$$

$$I = \frac{b_c t_c^3}{12}; y = \frac{t_c}{2}$$

$$t_c = \sqrt{\frac{6 \times M_b}{b_c \times \sigma_b}}$$

$$\sigma_b = 0.5 \times \sigma_y = 125 \text{ MPa}$$

b_c : The cap width; equals crank pin length

t_c : The cap thickness

σ_b : Permissible bending stress for the cap

σ_y : The yield strength for the cap

$$t_c = \sqrt{\frac{6 \times M_b}{b_c \times \sigma_b}} = \sqrt{\frac{6 \times 21469.33}{15 \times 125}} = 8.3 \text{ mm}$$

The width of the cap is 10 mm.

Connecting rod dimensions:

- | | |
|---|--------|
| 1. Connecting rod length | 145 mm |
| 2. Thickness of the cross-section | 2 mm |
| 3. Connecting rod breadth | 8 mm |
| 4. Connecting rod height at the small end | 10 mm |
| 5. Connecting rod height at the big end | 12 mm |
| 6. Small eye diameter | 12 mm |
| 7. Big eye diameter | 15 mm |
| 8. Cap thickness | 10mm |

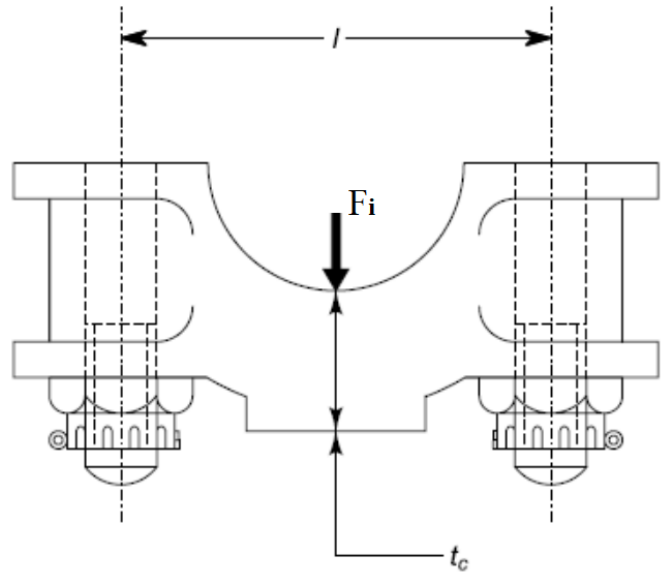


Fig 6: The force acting on the cap

3.4.4 Testing the crank shaft design using finite element method

The dimensions from the analytical solution are tested using the finite element method in the SolidWorks 2018 software to insure the safety of the connecting rod against buckling.

Table 1 shows the properties of the material used in this study.

Material Properties	
Name	: AISI 1045 Steel, cold drawn
Model type	: Linear Elastic Isotropic
Default failure criterion	: Max von Mises Stress
Yield strength	: 5.3×10^8 N/m ²
Tensile strength	: 6.25×10^8 N/m ²
Elastic modulus	: 2.05×10^{11} N/m ²
Poisson's ratio	: 0.29
Mass density	: 7850 kg/m ³
Shear modulus	: 8×10^{10} N/m ²
Thermal expansion coefficient	: 1.15×10^{-5} /Kelvin

Table1: the mechanical properties of AISI 1045.

First step in the numerical solution is to create a model of the connecting rod then generating the mesh. A model of the connecting rod was drawn SolidWorks 2018. Figure 7 and 8 show the model before and after the mesh was generated. The boundary conditions are then defined. In our study, the face of the big end in contact with the crank pin is set to be fixed while the force is applied on the surface of the small end in contact with the piston pin.

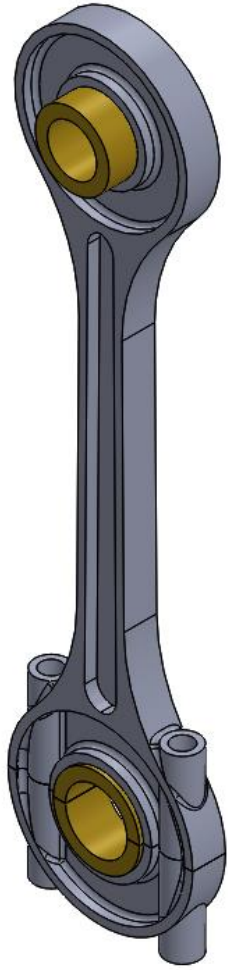


Figure 7: A model of the connecting rod



Figure 8: The model after mesh is generated

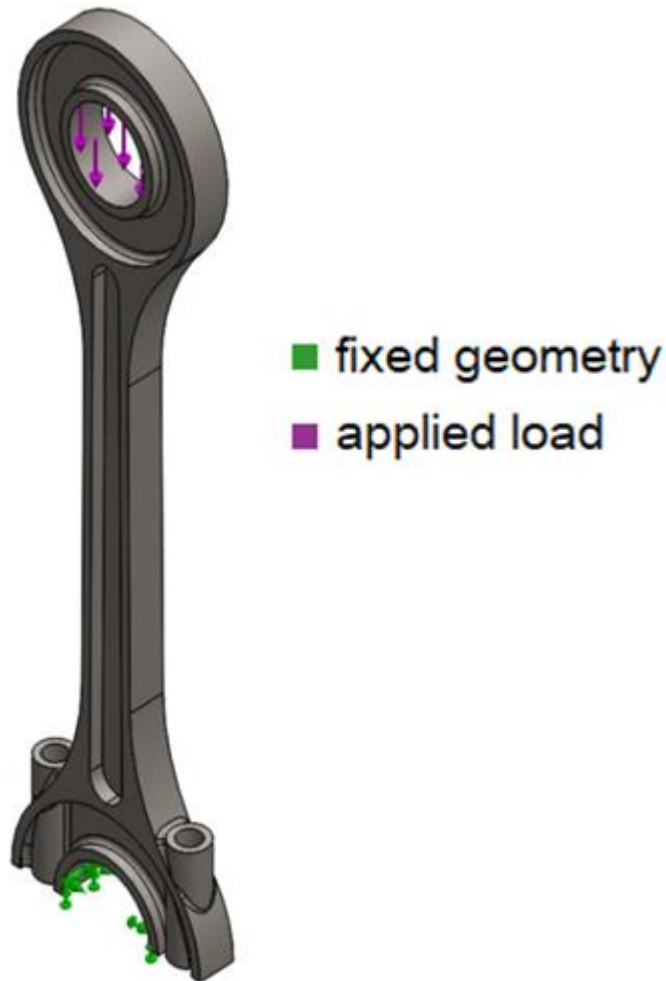
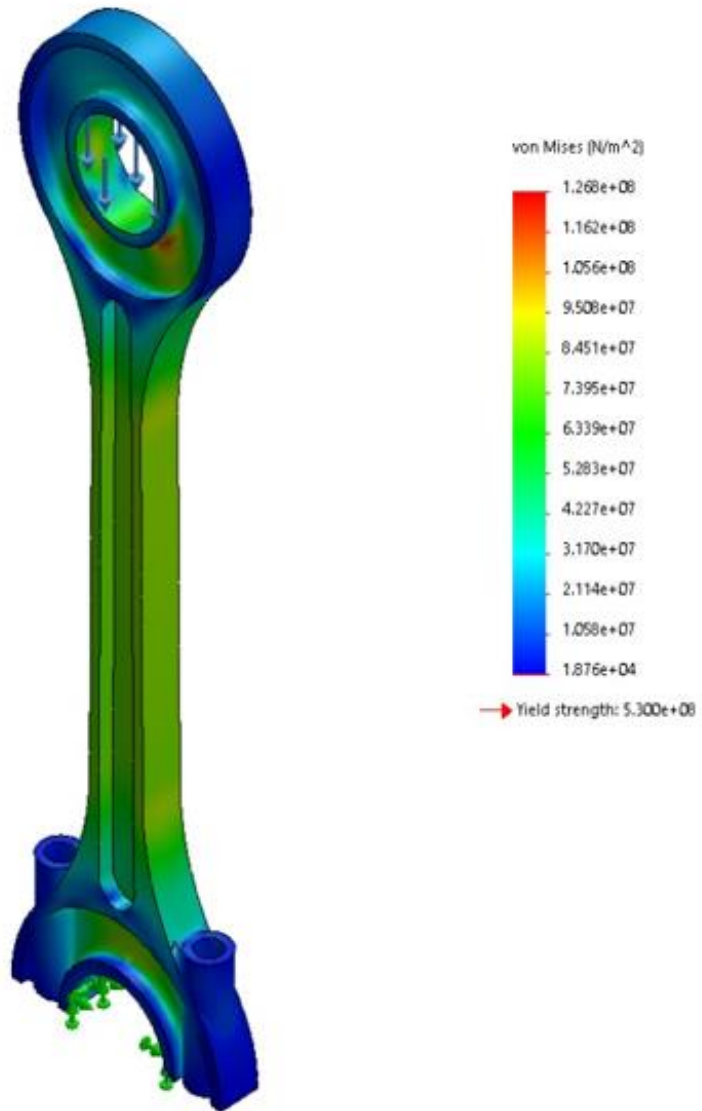


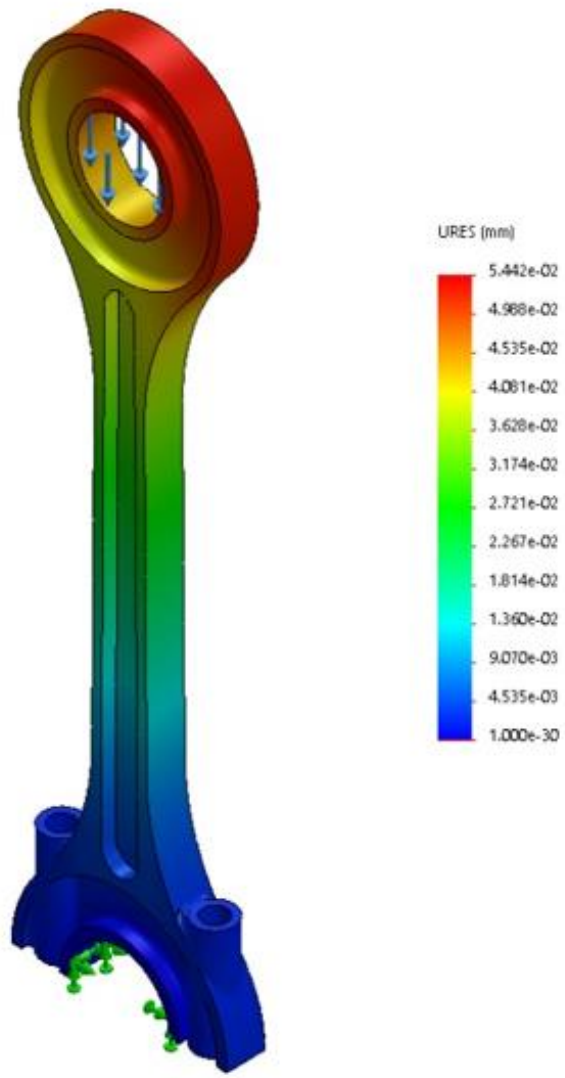
Figure 9: the boundary condition defined on the connecting rod

Figures 10, 11 and 12 show the result for the stresses on different portions of the connecting rod, the connecting rod deformation and the strain respectively. The maximum stress is less than the allowable stress for the material. The maximum, deformation is $5.442e-02$ mm which is very small. The connecting rod will keep its shape since the maximum strain is a very small, $4.523e-04$.



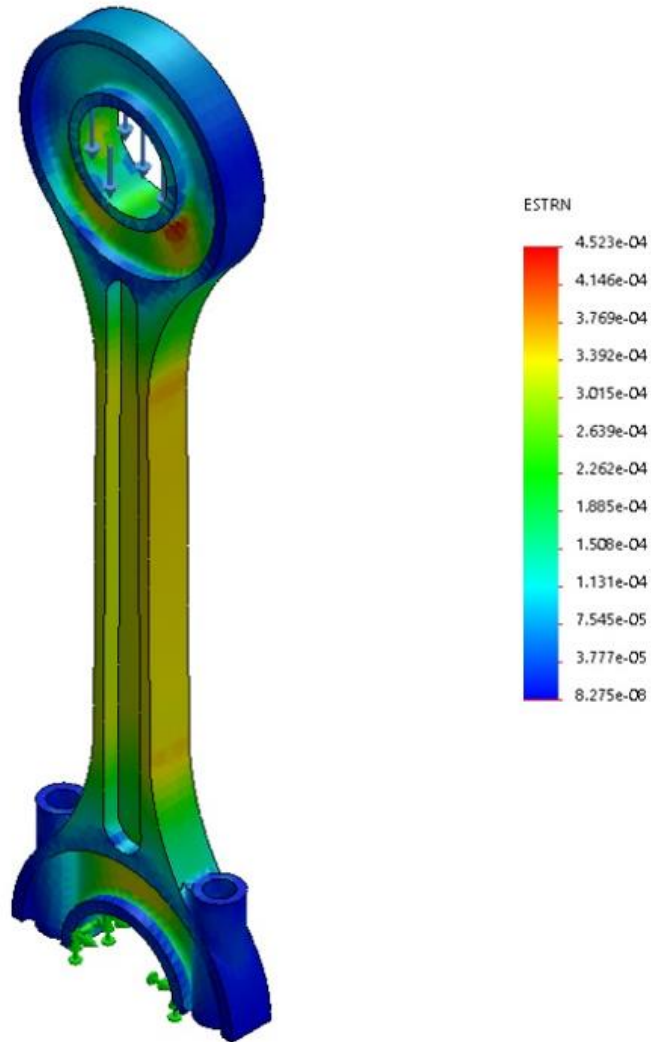
connecting rod-stress result

Fig 10: stresses on the connecting rod



connecting rod-deformation result

Fig 11: deformation of the connecting rod



connecting rod-strain result

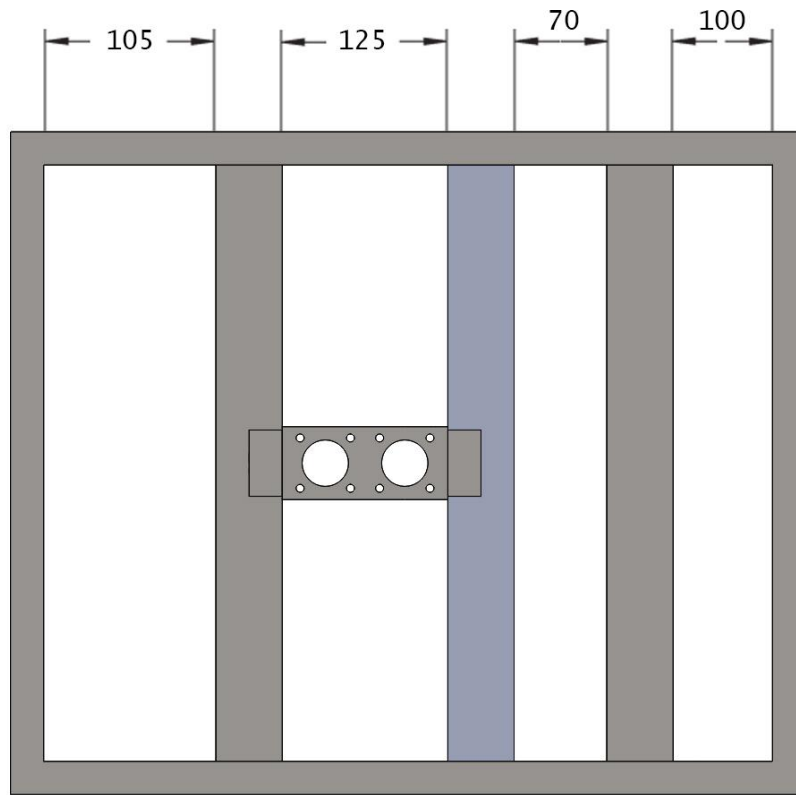
Fig 12: strain of the connecting rod

3.5 Chassis design

The chassis is the metal parts that connects allow components and systems of the vehicle together. It is made of mild steel AISI 1015(3.07 kg/m). 50x25x3 mm rectangular tube cross section was used to reduce the weight of the vehicle.

The dimension of the cross section of the chassis were chosen arbitrary and tested for stresses. Considering the dimensions of all components and allowances, the chassis measures 450 mm in width and 600 mm in length.

The pneumatic actuators are bolted on mild steel rectangular bar.



top view

Fig: Top view of the chassis

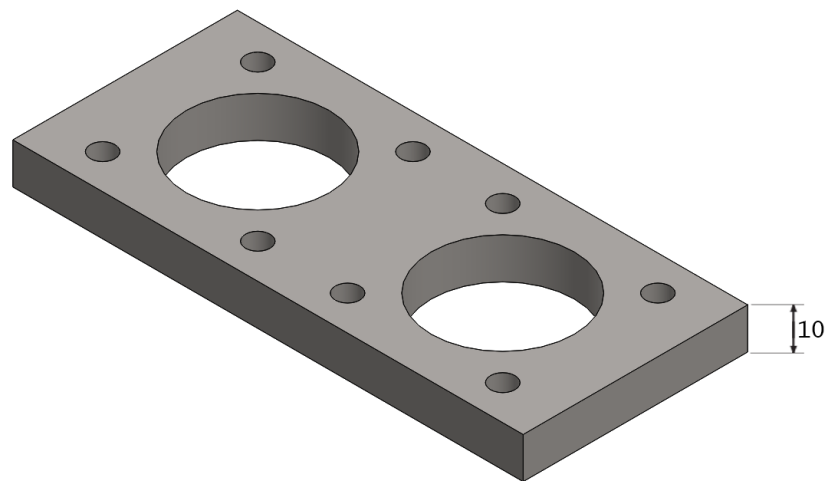


Fig: Isometric view of the bar holing the pneumatic actuators

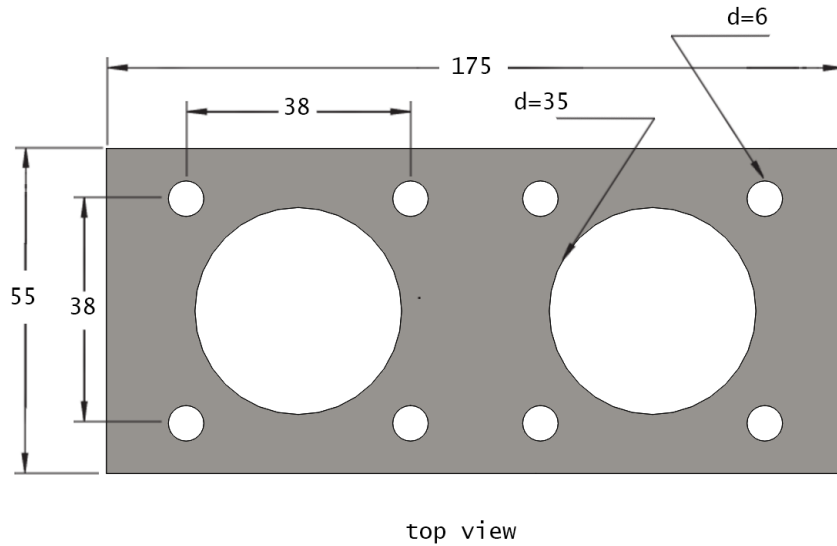


Fig: Top view of the bar holing the pneumatic actuators

To confirm the safety of the chassis design, the beam carrying the maximum load was analyzed using finite element method in SolidWorks 2018.

The maximum load is applied on the beam beneath the air tank due to the mass of the air in the tank. The analysis also includes the weight of the beam.

The table below shows the properties of the steel used for manufacturing the chassis.

Material Properties	
Name:	AISI 1015 Steel, Cold Drawn (SS)
Model type:	Linear Elastic Isotropic
Default failure criterion:	Max von Mises Stress
Yield strength:	3.25e+08 N/m ²
Tensile strength:	3.85e+08 N/m ²
Elastic modulus:	2.05e+11 N/m ²
Poisson's ratio:	0.29
Mass density:	7870 kg/m ³
Shear modulus:	8e+10 N/m ²
Thermal expansion coefficient:	1.2e-05 /Kelvin

Table: properties of the chassis material

Model name: Part1
(Default name) (Default)
Mesh type: Solid Mesh

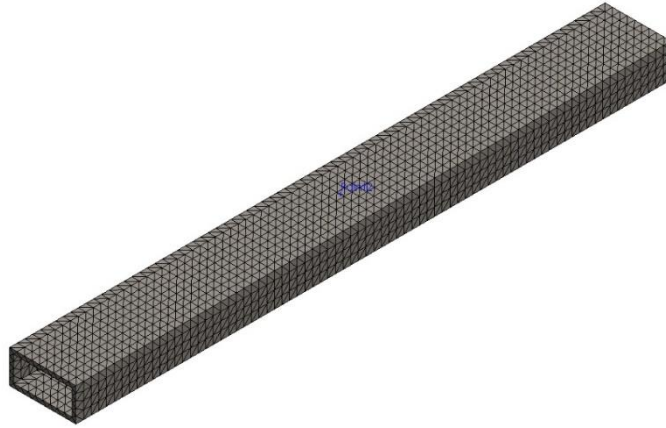


Fig: a model of the beam carrying the maximum load after mesh generation

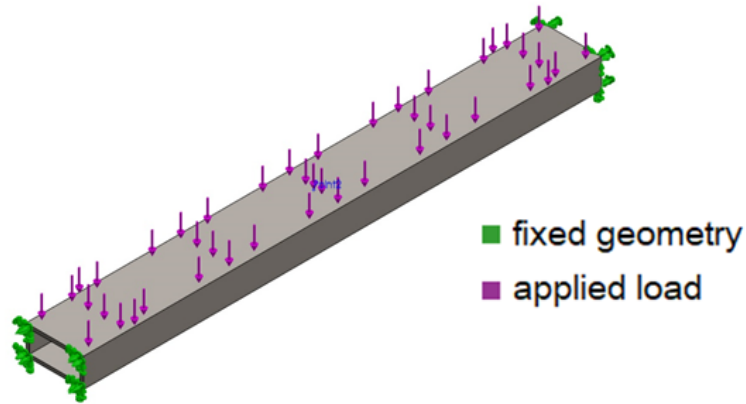
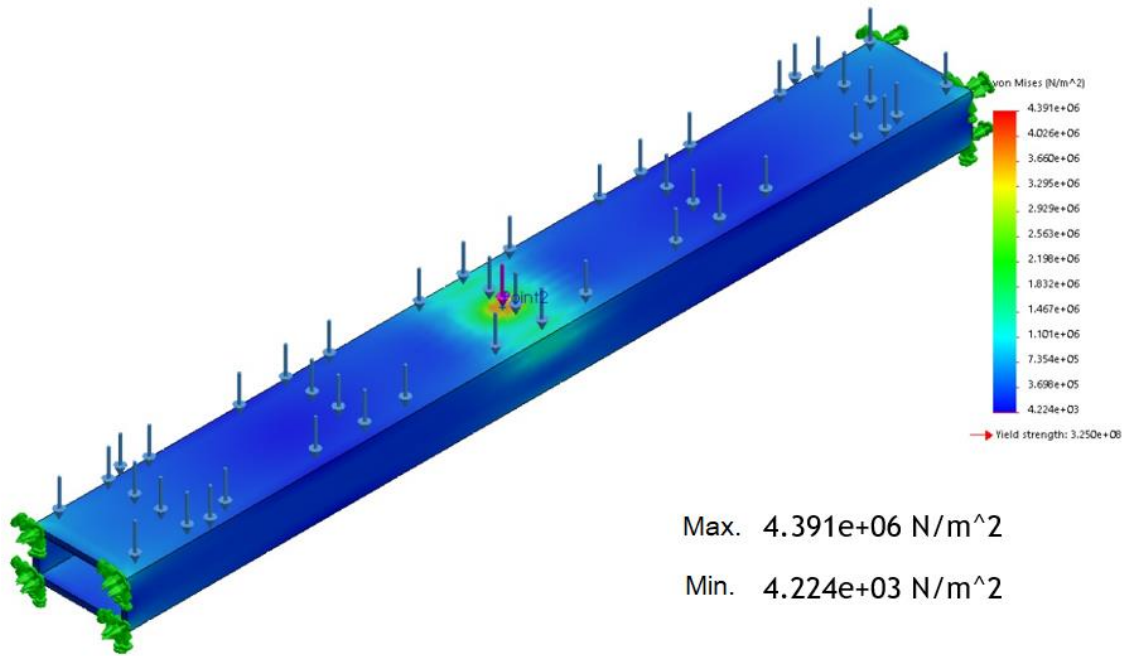


Fig: The boundary conditions applied to the beam carrying the maximum load

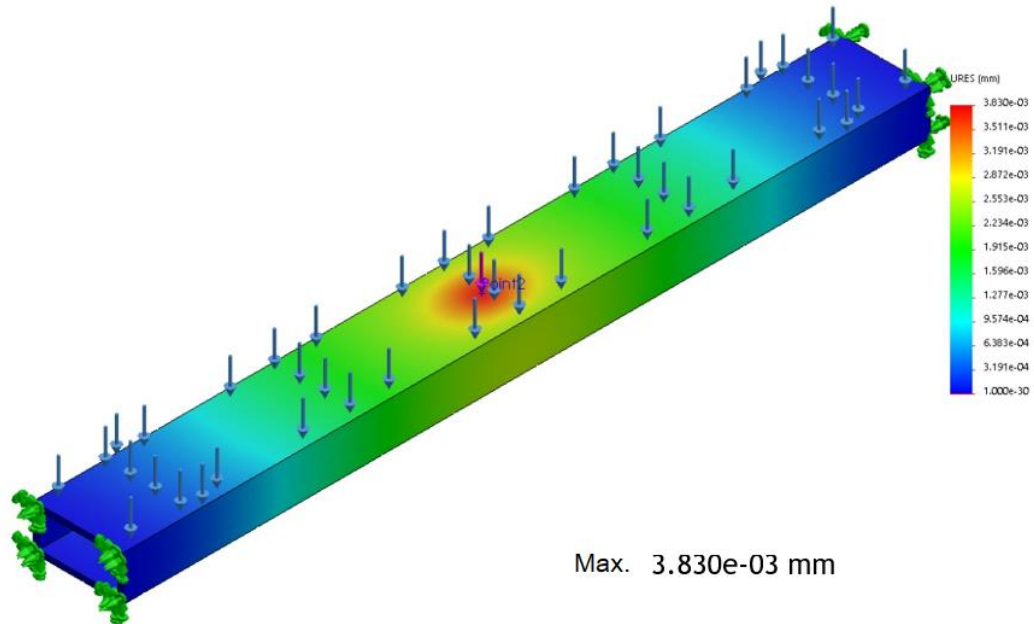
The results of this analysis are shown in the following figures. As we can see, the stresses, deformation and the strain values represent a secure design.



Max. 4.391e+06 N/m²

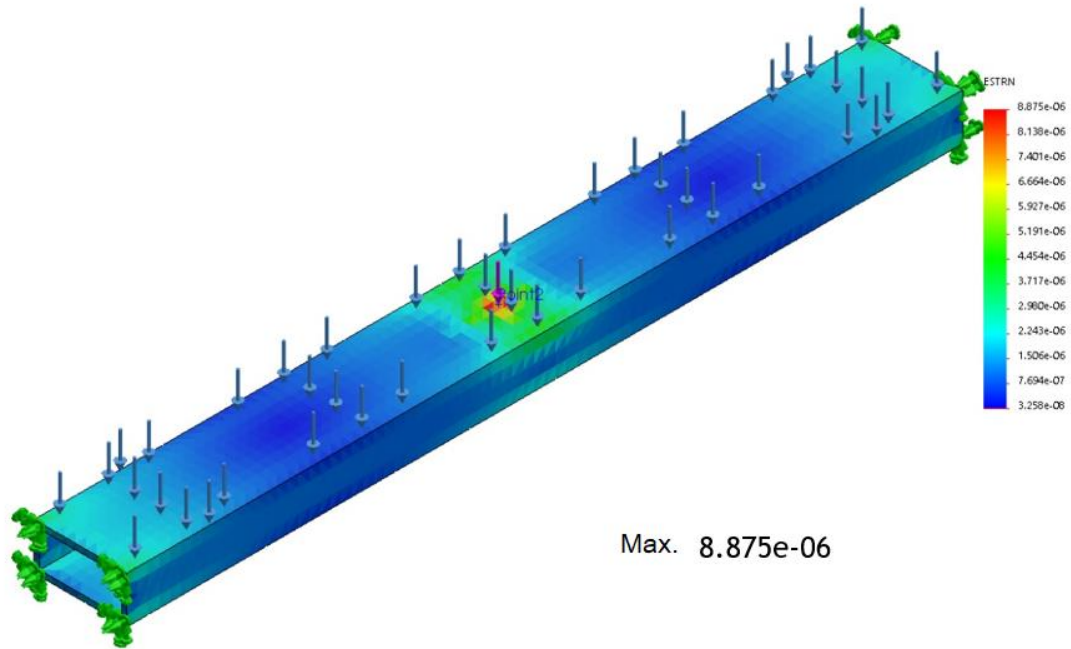
Min. 4.224e+03 N/m²

Stress



Max. 3.830e-03 mm

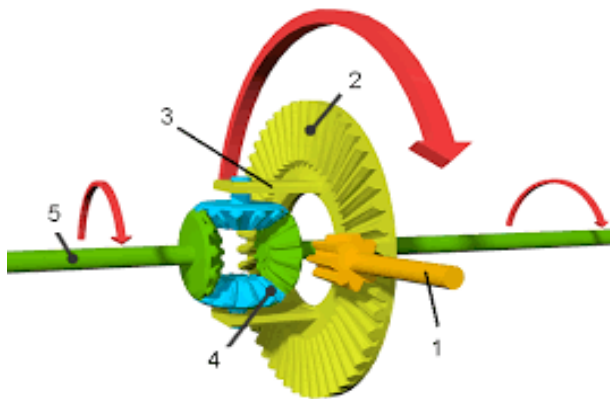
deformation



Strain

3.6 Differentials

Differentials is a system that transmits an engine's torque to the wheels. The differential takes the power from the engine and splits it, allowing the wheels to spin at different speeds. Each wheel is able to turn independently from the other such as when the car is turning. The differentials assembly consists of a pinion gear attached to the propeller shaft, bevel gear, connecting edge, and side gear in addition to left and right axle shafts.



- 1: pinion gear and the propeller shaft
- 2: bevel gear
- 3: connecting edge
- 4: side gear
- 5: left axle shaft
- 6: right axle shaft

Fig: The differentials assembly

Input parameters

$$\text{Gear ratio} = \frac{t_{\text{out}}}{t_{\text{in}}} = \frac{N_{\text{in}}}{N_{\text{out}}} = \frac{T_{\text{out}}}{T_{\text{in}}} \quad (t = \text{NO of teeth: } N = \text{rotational speed: } T = \text{torque}) = 32/8 = 4$$

$$\text{Input power} = \frac{2 \cdot 3.14 \cdot N_A \cdot T_A}{60} = 62.8 \text{ W (PI)}$$

$$\text{Output power} = \eta (\text{efficiency}) \cdot P_{\text{in}} = 0.85 \cdot 62.8 = 53.38 \text{ W (PO)}$$

Input torque 10 NM (T_i) expected value

$$\text{Output torque} = T_B = \frac{60 \cdot P_{\text{out}}}{2 \cdot 3.14 \cdot N_B} = 33.9827 \text{ W so the } T_B \text{ ideal} = 33.98 = \text{so the (the torque actual)} = \text{ideal torque} \cdot \eta = 33.98 \cdot 0.85 = 28.883 \text{ that's the actual value}$$

Input speed 60rpm (N_A) same as the shaft rotation speed

$$\text{Output speed: } GR = \frac{N_{\text{in}}}{N_{\text{out}}} \text{ so } N_o = 60/4 = 15\text{rpm}$$

$$\text{Module} = \text{pitch diameter} / \text{number of teeth} = 1$$

The material used for the pinion and gear is medium carbon steel whose allowable bending stress maybe taken as 230 MPA where modulus elasticity taken as 210GPA

Design of inner bevel

Pitch geometry (D) 15 mm

Pitch cone angle (Y) 45

Back cone angle (B) 45

Pressure angle 20

Module 2 mm

Velocity ratio 1

Inner bevel set

Pitch cone distance (AO)

$$= \sqrt{\left(\frac{D_1}{2}\right)^2 + \left(\frac{D_2}{2}\right)^2} = \text{where } D_1 = D_2 = 20 \quad AO = 6.32 \text{ mm}$$

Face width (b)

$$B = \frac{AO}{3} = 6.324/3 = 2.108\text{mm}$$

Height addendum

$$H_a = 1 \cdot m = 1 \cdot 2 = 2\text{mm}$$

Height of Dedendum (hf)

$$H_f = 1.25 * m = 1.25 * 2 = 2.5$$

$$\text{Mean radius (R mean)} = (D/2) - (b/2) \sin Y = (20/2) - (3.726/2) \sin 45 = 8.42 \text{ mm}$$

$$\text{Minimum number of teeth (zmin)} = \frac{2 * 2 \cos(45)}{m(\cos 20)^2} = 4.9 \text{ near to } 5 = 5 \text{ teeth}$$

So the actual number of teeth $D = m * Z = 10/2 = 5$

Since the $Z_{\text{actual}} = Z_{\text{min}}$ so it's permissible

Force analysis of inner bevel set

$$\text{Tangential force (FT)} = T/R_{\text{mean}} = 28.875/15 = 1.925 \text{ NM}$$

$$\text{Radial force on pinion FR} = FT * \tan(Y) * \cos(45) = 2.2629 \text{ N}$$

Pitch line velocity

$$V_m = \frac{3.14 * D * N}{60000} \text{ (where D is the mean diameter} = 2 * R_{\text{mean}}) = 0.0132 \text{ m/s}$$

Equivalent teeth on pinion

$$Z_{ep} = Z_p / \cos(45) * \text{soc}(45) \text{ power } 3 = 5 / \cos 45 * \cos 45 \text{ power } 3 = 66 \text{ teeth}$$

$$\text{So we have to find the Lewis factor (Y)} = .921 / Z_{ep} = .154 \text{ (}.921/66) = .141$$

So the material selection is alloy steel-15Ni4Cr1

$$S_{ut} \text{ (ultimate strength stress in shear)} = 1500 \text{ NMM}^2$$

$$\text{BHN} = 650$$

Safety factor shall be considered as 1.5

σ_a = allowable bending stress

$$= S_{ut} / 3 = 1500 / 3 = 500 \text{ N/MM}$$

Stress based analysis of inner bevel set

$$S_b = \sigma_a * C_v * b * 3.14 * m * Y * \frac{A_o_b}{A_o}$$

$$= 500 * .7462 * 2.108 * 3.14 * 2 * .141 * .665 = 463.122 \text{ N}$$

The ratio factor is 1 meter gears

Shear stress on hollow bevel drive shaft

$$\text{Inner diameter (di)} = 15 \text{ mm}$$

$$\text{Outer diameter (do)} = 23 \text{ mm}$$

The permissible shear stress = $\frac{.5 \text{ Sut}}{\text{FOS}} = 500 \text{ N/MM}^2$

The actual shear stress = $\frac{16T}{3.14 * D^3 * (1_c^4)} = 33.95$

Since the actual shear is less than the permissible one so design is permissible

Sun gear parameters

Module=2

Teeth=32

Pressure angle=20

Face width=2.108mm

Hub diameter=18mm

Mounting distance=32mm

Nominal shaft diameter=13mm

Pinion gear

Teeth=8

Pressure angle=20

Face width=2.108

Hub diameter=12

Nominal shaft diameter=10mm

Mounting distance=32

Crown gear

Module=2

Teeth 32

Pressure angle=20

Face width=2.108mm

Hub diameter=40mm

Nominal diameter=20mm

Mounting distance=25mm

Driving gear

M=2

Teeth=8

Pressure angle=45

Face width=2.108mm

Hub diameter=20mm

Mounting distance=50mm

Nominal shaft diameter=15mm

3.7 bearings design

Bearings are made of hard steel that guide and support shafts and axles. They are part of the chassis, guide the wheels and absorb axial and radial forces. Radial forces are longitudinal forces produced as a result of rotation. They are applied to the bearing at a right angle to the longitudinal axis.

Essentially, ball bearings consist of

- Outer and inner rings
- The rolling elements
- A ball cage enclosing the rolling elements.

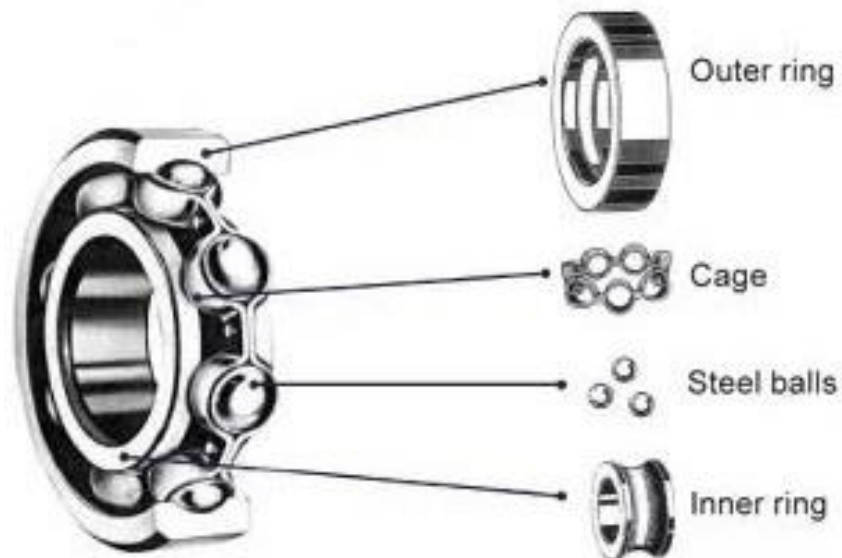
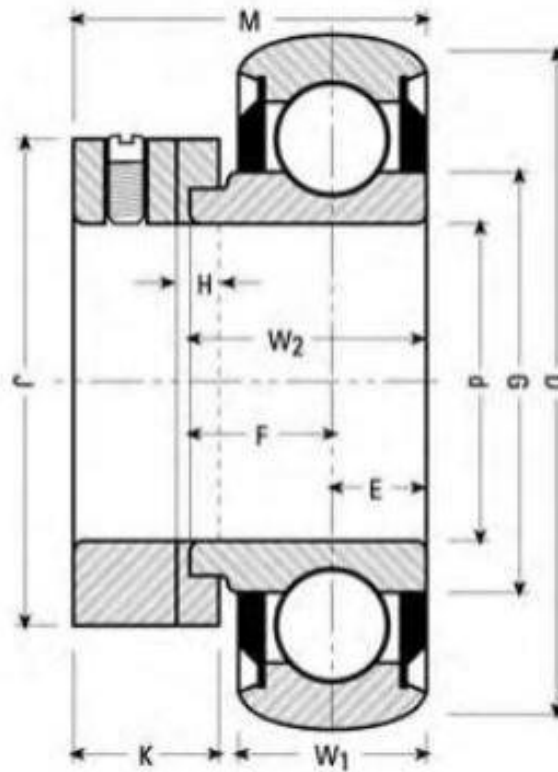


Fig: construction of ball bearings

Commercial 306s roller bearings were used for the wheels and the crank shaft. The following figures shows the dimensions of the used bearings.



"NPS" Series

Spherical O.D.	Basic Outer Ring	Bore d Inch	O.D. D mm	Inner W2 mm	Outer W1 mm	E	F	G	H Inch	J	K	M	R	Collar		
NPS-008-RRC	203	1/2	40	1.575	0.750	13	0.512	0.256	0.494	0.957	0.156	1.125	0.531	1.125	0.126	C008
NPS-010-RRC	203	5/8	40	1.575	0.750	13	0.512	0.256	0.494	0.957	0.156	1.125	0.531	1.125	0.126	C010

Fig: Dimensions of the ball bearing

These bearing are from Motions Industries. The model NPS-008-RRC is used to reduce the friction between the wheels shaft and the chassis. While NPS-010-RRC is used for the crankshaft.

CONCLUSION

This project presented a secure mechanical design of a vehicle that exploits the natural air to move. Using the compressed air produces zero emissions and reduces the vehicle manufacturing cost since some systems will not be necessary e.g. cooling system, starter motor etc. so we can say the objectives of this study were achieved. However, the limited storage capacity of the air tank remains a major drawback.

References

- (1) Daniel A. Vallero, Fundamentals of Air Pollution, 5th Ed.
- (2) Kenneth Wark-Cecil F. Warner-Wayne T. Davis, Air Pollution: its origin and control, 3rd Ed.
- (3) Aqib Mehmood – Hazrat Bilal , Design Simulation and Fabrication of Vehicle Exhaust Gas Emission Control System (Smart Exhaust Technology)
- (4) Bolaji and S.B. Adejuyigbe, VEHICLE EMISSIONS AND THEIR EFFECTS ON NATURAL ENVIRONMENT – A REVIEW , Journal of the Ghana Institution of Engineers Vol. 4, No.1, 2006, pp 35–41
- (5) Ioannis Manisalidis, Elisavet Stavropoulou, Agathangelos Stavropoulos and Eugenia Bezirtzoglou , Environmental and Health Impacts of Air Pollution: A Review
- (6) Website : www.ijsrp.org/research-paper-0717/ijsrp-p6747.pdf
- (7) Website : www.sciencedirect.com/science/article/pii/S2351978920309446
- (8) Website www.sciencedirect.com/science/article/pii/S187770581400890X
- (9) JDSII , Remote Controlled Pneumatic Cylinder
- (10) Website: <https://community.createlabz.com/knowledgebase/wireless-control-nrf24l01-of-servo-motors-using-joystick-module/>
- (11) Muslim Ali, Design of the Crankshaft, researchgate.net , May 2020
- (12) D. CHANAKYA GUPTA, CHAITANYA JOSHI, B RAMAKRISHNA, DESIGN AND ANALYSIS OF CRANK SHAFT , INTERNATIONAL JOURNAL OF PROFESSIONAL ENGINEERING STUDIES, Volume VIII /Issue 5 / AUG 2017
- (13) Muslim Ali, Design of connecting rod, researchgate.net , May 2020
- (14) Richard G. Budynas, J. Keith Nisbett, Shigley’s Mechanical Engineering Design, 10th Ed.